

Spectral properties of noisy classical and quantum propagators

Stéphane Nonnenmacher

May 22, 2019

Abstract

We study classical and quantum maps on the torus phase space, in the presence of noise. We focus on the spectral properties of the noisy evolution operator, and prove that for any amount of noise, the quantum spectrum converges to the classical one in the semiclassical limit. The small-noise behaviour of the classical spectrum highly depends on the dynamics generated by the map. For a chaotic dynamics, the outer spectrum consists in isolated eigenvalues (“resonances”) inside the unit circle, leading to an exponential damping of correlations. On the opposite, in the case of a regular map, part of the spectrum accumulates along a one-dimensional “string” connecting the origin with unity, yielding a diffusive behaviour. We finally study the non-commutativity between the semiclassical and small-noise limits, and illustrate this phenomenon by computing (analytically and numerically) the classical and quantum spectra for some maps.

Introduction

Numerical studies of chaotic dynamical systems inevitably face the problem of rounding errors due to finite computer precision. Indeed, the instability of the dynamics would require an infinite precision of the initial position, if one wants to compute the long-time evolution. Besides, any deterministic model describing the evolution of some physical system is intrinsically an approximation, which neglects unknown but presumably small interactions with the “environment”. A way to take this interaction into account is to introduce some randomness in the deterministic equations, for instance through a term of Langevin type. Such a term induces some diffusion, that is, some coarse-graining or smoothing of the phase space density. If the deterministic part of the dynamics is unstable, it has the opposite effect to transform long-wave-length fluctuations of the density into short-wave-length ones, so the interplay between both components (deterministic vs. random) of the dynamics is

Service de Physique Théorique, CEA/DSM/PhT Unité de recherche associée au CNRS CEA/Saclay 91191 Gif-sur-Yvette cédex, France. e-mail:nonnen@sph.t.saclay.cea.fr

a priori not obvious. Rigorous results on the behaviour of noisy hyperbolic systems have been obtained recently [21, 5, 7]: they show that a major property of deterministic hyperbolic systems, namely the exponential mixing, still holds in presence of noise. Actually, introducing some noise provides a way to compute the exponential decay rate (and the subsequent “resonances”) in a controlled fashion (cf. the numerical study of [1]).

In quantum mechanics, a (small) system is never perfectly isolated either, and is subject to inevitable interaction with the environment, responsible for decoherence effects. The study of decoherence has received a large attention recently, due to the (mostly theoretical) interest in quantum computation [13] and precise experiments measuring decoherence. In some simple cases, one can study the dynamics of the full system (small plus environment), and obtain an effective dynamics of the small one [11]. Under suitable assumptions, this effective dynamics results in a memoryless (super)operator acting on the quantum density of the small system.

A possible way to modelize this operator is by quantizing the “Langevin term” used in the classical framework, that is introduce a random noise in the quantum evolution equation (for either continuous or discrete time dynamics). Averaging over the noise yields, in the continuous-time framework, a non-Hermitian “Lindblad operator” [25], while in the discrete-time case the evolution can be cast into the product of a unitary (deterministic) evolution operator with a “quantum coarse-graining” operator [6], this product being called from now on the “coarse-grained evolution operator”. Similar operators have also appeared in the theoretical study of spectral correlations for quantized maps [28].

Several recent studies have been devoted to noisy or coarse-grained quantum maps [22, 26, 6] in the semiclassical limit, emphasizing the respective roles of regular vs. chaotic regions in the classical phase space. The aim was either to study the time evolution of an initial density [6], or to compute the spectrum of the classical or quantum coarse-grained evolution operators [22, 26].

In this paper, we present some results on the latter (spectral) problem, for maps defined on the 2-torus (Section 1). For the sake of simplicity, we restrict ourselves to either fully chaotic or fully regular maps. In the limit of vanishing noise, the spectrum of the classical coarse-grained evolution operator behaves differently in these two (extreme) cases: for a chaotic map, the spectrum has a finite gap between unity and the next largest eigenvalue, due to exponential decay of correlations [7], while in the regular case some eigenvalues come arbitrary close to unity. To illustrate these results, we study in detail some linear systems (either chaotic or integrable), for which the eigenvalues may be computed analytically.

We then turn to the associated quantized systems (Section 3). After recalling the setting of quantum maps on the torus, we define the quantum coarse-graining operator, and then prove that for any classical map and a fixed finite noise, the spectrum of the quantum coarse-grained evolution operator converges to the spectrum of the classical one in the semiclassical limit (Theorem 1).

We finally study in Section 4 the non-commutativity of the semiclassical vs. vanishing-noise limits, using as examples the maps studied in the classical framework (Section 4). As a byproduct, we show that one can obtain the resonances of a classical hyperbolic map from the spectrum of an associated quantum operator (the quantum coarse-grained propagator),

provided the coarse-graining is set to decrease slowly enough in the semiclassical limit (we conjecture a sufficient condition for the speed of convergence). On the opposite, for an integrable map the same limit yields a spectrum densely filling one-dimensional curves (“strings”) in the unit disk, one of them containing unity as a limit point.

1 Classical noisy evolution

The classical dynamical systems we will study are defined on a 2-dimensional symplectic and Riemannian manifold, the torus $\mathbb{T}^2 = \mathbb{R}^2/\mathbb{Z}^2$. The maps are smooth (C^1), invertible and leave the symplectic form $d\mathbf{p} \wedge d\mathbf{q}$ (and therefore the volume element $d^2\mathbf{x} = d\mathbf{q}d\mathbf{p}$) invariant: they are canonical diffeomorphisms of \mathbb{T}^2 . Such a map $\mathbf{x} = (\mathbf{q};\mathbf{p}) \mapsto \mathbf{M}\mathbf{x}$ naturally induces a *Perron-Frobenius operator* $\mathbb{P} = \mathbb{P}_{\mathbf{M}}$ acting on phase space densities $\rho(\mathbf{x})$: $\mathbb{P}\rho(\mathbf{x}) = \rho(\mathbf{M}^{-1}\mathbf{x})$.

1.1 Spectral properties of the classical propagator

In this section we review the spectral properties of the Perron-Frobenius operator $\mathbb{P}_{\mathbf{M}}$, depending on the map \mathbf{M} and on the functional space on which the operator acts. The results presented are not new, but allow us to fix some notations.

1.1.1 Spectrum on $L^2(\mathbb{T}^2)$

For any canonical diffeomorphism \mathbf{M} and any $\rho \geq 0$, the spectrum of $\mathbb{P}_{\mathbf{M}}$ on the Banach space $L^1(\mathbb{T}^2)$ is a subset the unit circle and admits $\int_{\mathbb{T}^2} \rho(\mathbf{x}) d^2\mathbf{x} = 1$ as invariant density. In particular, \mathbb{P} is unitary on $L^2(\mathbb{T}^2)$ and on its subspace \mathcal{L}_0 of zero-mean densities.

One can relate some dynamical properties of the map \mathbf{M} with the (unitary) spectrum of \mathbb{P} on \mathcal{L}_0 [14]. For instance, if the dynamics \mathbf{M} leaves invariant an observable $H(\mathbf{x}) \in \mathcal{L}_0$ (e.g. if \mathbf{M} is the stroboscopic map of the Hamiltonian flow generated by H), then all observables of the type $\rho(\mathbf{x}) = f(H(\mathbf{x}))$ are invariant as well, so that the eigenvalue 1 of \mathbb{P} is infinitely degenerate. The full spectrum of \mathbb{P} will be explicitly given for some integrable maps in section 2.2.

On the opposite, the map \mathbf{M} is ergodic iff \mathbb{P} has no invariant density in \mathcal{L}_0 (i.e. if 1 is a simple eigenvalue in L^2). Stronger chaotic properties may be defined in terms of the *correlation function* between two densities $f, g \in \mathcal{L}_0$:

$$C_{fg}(t) \stackrel{\text{def}}{=} \int_{\mathbb{T}^2} d\mathbf{x} f(\mathbf{x})g(\mathbf{M}^{-t}\mathbf{x}) = \langle f; \mathbb{P}^{-t}g \rangle \quad (1)$$

(the time parameter t will always take *integer* values). The map \mathbf{M} is said to be *mixing* iff for any f, g , the correlation function behaves for large times as:

$$C_{fg}(t) \xrightarrow{t \rightarrow \infty} \int_{\mathbb{T}^2} d\mathbf{x} f(\mathbf{x}) \int_{\mathbb{T}^2} d\mathbf{x} g(\mathbf{x}) \quad (2)$$

A slightly weaker property (weak mixing) is equivalent with the fact that $\mathbb{P}_{\mathbf{M}}$ has no eigenvalue in \mathcal{L}_0 .

1.1.2 Exponential mixing

For a certain class of maps (e.g. the Anosov maps defined below), the convergence of mixing is exponentially fast, provided the observables $f, g \in C^k(\mathbb{R}^n)$ are smooth enough. One speaks of *exponential mixing* with a decay rate $\lambda > 0$ if $\int_{\mathbb{R}^n} f(x)g(T^t(x))dx - \int_{\mathbb{R}^n} f(x)dx \int_{\mathbb{R}^n} g(x)dx = O(e^{-\lambda t})$ for a certain constant $K_{f,g}$.

This behaviour can sometimes be explained through the spectral analysis of the Perron-Frobenius operator P acting on an *ad hoc* functional space B , with $B \subset L^2$ (in general B contains some distributions). One proves that the operator P on B is *quasi-compact*: its spectrum consists of finitely many isolated eigenvalues λ_i (called *Ruelle-Pollicott resonances*) situated in an annulus $r < \lambda_i < 1$ for some $r > 0$, plus possible essential spectrum inside the disk of radius r . In that case, assuming for simplicity that each λ_i is a simple eigenvalue with spectral projector E_i , the spectral decomposition of P on B leads to the following asymptotic expansion for $C_{f,g}(t)$ in the limit $t \rightarrow \infty$:

$$C_{f,g}(t) = \sum_i \lambda_i^t \langle f, E_i g \rangle + O(r^t) \quad (3)$$

In the above expression, the brackets do not refer to a Hermitian structure, but represent the integrals $\int_{\mathbb{R}^n} f(x)E_i g(x)dx$. The first resonance $\lambda_0 = 1$ corresponds to the unique invariant density ρ_0 , and the decay rate (obviously independent of the observables f, g) is given by $-\log |\lambda_1|$ resp. by $-\log r$ if there is no resonance other than unity.

This type of spectrum was first put in evidence in the case of uniformly hyperbolic maps by using Markov partitions of the phase space and translating the dynamics on the phase space into a simple symbolic dynamics [34]. It was later extended to more general systems, including non-uniformly hyperbolic ones. In the next sections, we will introduce the Anosov diffeomorphisms on the torus, which often serve as “model” for deterministic chaos.

1.1.3 Anosov diffeomorphism on the two-dimensional torus

In this section we recall the definition and some properties of an Anosov diffeomorphism M on the torus T^2 [19]. The Anosov property means that at each point $x \in T^2$, the tangent space $T_x T^2$ splits into $T_x T^2 = E_x^s \oplus E_x^u$, where $E_x^{u=s}$ are the local stable and unstable subspaces. The tangent map $d_x M$ sends $E_x^{u=s}$ to $E_{M(x)}^{u=s}$, and there exist constants $A > 0$; $0 < \lambda_s < 1 < \lambda_u$ (independent on x) s.t.

$$\|d_x M^{-t}|_{E_x^s}\| \leq A \lambda_s^{-t} \quad \text{and} \quad \|d_x M^{-t}|_{E_x^u}\| \leq A \lambda_u^{-t} \quad (4)$$

These inequalities describe the uniform hyperbolicity of M on T^2 . The splitting of $T_x T^2$ into $E_x^{u=s}$ has in general regularity $C^{1+\alpha}$ for some $1 > \alpha > 0$, meaning that it is differentiable and its derivatives are Hölder-continuous with coefficient α .

This uniform hyperbolicity implies that M is ergodic w.r.to the Lebesgue measure on T^2 , and exponentially mixing (see next section).

A simple example of such diffeomorphisms is provided by the linear hyperbolic automorphisms of \mathbb{T}^2 , defined by matrices $A \in \text{SL}(2; \mathbb{Z})$ with $|\text{tr} A| > 2$. These maps are sometimes referred to as “generalized cat maps”, in reference to Arnold’s “cat map” $A_{\text{Arnold}} = \begin{pmatrix} 2 & 1 \\ 1 & 1 \end{pmatrix}$.

[3]. We will study in some detail these linear maps and their quantizations, since one can obtain very explicit description of the associated coarse-grained propagators. One can perturb the linear hyperbolic automorphism A with the stroboscopic map $\rho_{\frac{1}{h}}$ generated by a Hamiltonian $H(\mathbf{x})$ on the torus: $M \stackrel{\text{def}}{=} \rho_{\frac{1}{h}} \circ A$. If the Hamiltonian H is “small enough”, then the perturbed map M remains Anosov.

1.1.4 Ruelle resonances for Anosov diffeomorphisms

As announced above, Anosov diffeomorphisms on \mathbb{T}^2 are exponentially mixing, and their correlation functions satisfy expansions of the type (3). Although the original proofs made use of Markov partitions and transfer operators associated with the symbolic dynamics [34], we will rather describe a more recent approach [7] based on phase space functions and distributions, which has the advantage to provide results for the coarse-grained propagator.

The authors of [7] define a Banach space \mathcal{B} of densities adapted to the map M : the space contains generalized functions which are smooth along the unstable direction of M but possibly singular (dual of smooth) along the stable direction. In particular, these functions are too singular to be in L^2 , which allows a non-unitary spectrum for \mathcal{P} on \mathcal{B} . The space \mathcal{B} is defined in terms of an arbitrary parameter $0 < \epsilon < 1$, and satisfies the continuous one-to-one embeddings: $C^1(\mathbb{T}^2) \hookrightarrow \mathcal{B} \hookrightarrow C^1(\mathbb{T}^2)$.

The space \mathcal{B} depends on the dynamics M , and also of the direction of time: although the map M is invertible, the dynamics of the operator \mathcal{P} on \mathcal{B} is *irreversible*, due to the structure of \mathcal{B} . The space $\mathcal{B}_{M^{-1}}$ adapted to the map M^{-1} is different from \mathcal{B}_M (and different from its dual \mathcal{B}' as well).

The authors indeed show that \mathcal{P} is quasicompact in \mathcal{B} , with essential spectral radius r_{ess} bounded above by $r_{\text{ess}} = \max(\epsilon^{-1}; \epsilon)$ (see Eq. (4) for the definition of r_{ess}). For any $1 > r > r_{\text{ess}}$, the spectrum of \mathcal{P} in the ring $R_r \stackrel{\text{def}}{=} \{f \in \mathcal{B} \mid \|f\|_r \leq 1\}$ consists in isolated eigenvalues, the Ruelle-Pollicott resonances $\lambda \in \mathbb{C}$. Therefore, a spectral expansion similar with (3) holds for any pair of observables $f, g \in \mathcal{B}$, which includes in particular observables in $C^1(\mathbb{T}^2)$ (the expansion might be slightly more complicated than (3) due to possible degeneracies).

Under stronger smoothness assumptions, namely for *real-analytic* Anosov maps in two dimensions, Rugh [35] constructed a transfer operator acting on observables real-analytic along the unstable direction, and “dual of analytic” along the stable one; he showed that this operator is *compact*, which means that the essential spectral radius vanishes in that case.

1.2 Coarse-grained classical propagator

In this section we precisely define the operator representing the effect of “noise” on the deterministic evolution of M . This operator is of diffusion type, it realizes a coarse-graining of the densities.

1.2.1 Classical diffusion operator

We consider a smooth probability density $K(\mathbf{x})$ on \mathbb{R}^2 with compact support. For simplicity, we also assume that $K(\mathbf{x}) = K(-\mathbf{x})$. From there, to any $\epsilon > 0$ corresponds a probability density on the torus, defined as $K_\epsilon(\mathbf{x}) = \frac{1}{2\pi\epsilon^2} \sum_{\mathbf{n} \in \mathbb{Z}^2} K\left(\frac{\mathbf{x} + \mathbf{n}}{\epsilon}\right)$. Due to the compact support of K , we see that for small enough ϵ and any $\mathbf{x} \in \mathbb{T}^2$ this sum has at most one nonvanishing term (for \mathbf{x} close to the origin). We define the coarse-graining operator D_ϵ on $L^2(\mathbb{T}^2)$ as the following convolution:

$$D_\epsilon f(\mathbf{y}) = \int_{\mathbb{T}^2} d\mathbf{x} K_\epsilon(\mathbf{y} - \mathbf{x}) f(\mathbf{x}) \quad (5)$$

D_ϵ is a self-adjoint *compact* operator on $L^2(\mathbb{T}^2)$, with discrete spectrum accumulating at the origin.

We define the Fourier transform on the plane as $\tilde{K}(\mathbf{j}) = \int_{\mathbb{R}^2} d\mathbf{x} K(\mathbf{x}) e^{2i\mathbf{j} \wedge \mathbf{x}}$, with the wedge product given by $\mathbf{j} \wedge \mathbf{x} = j_1 x_2 - j_2 x_1$. From the assumptions on the density K , the function $\tilde{K}(\mathbf{j})$ is a real, even, smooth function, which takes its maximum at $\mathbf{j} = 0$ (where it behaves as $\tilde{K}(\mathbf{j}) = 1 - Q(\mathbf{j}) + o(|\mathbf{j}|^4)$, with $Q(\cdot)$ a positive definite quadratic form), and decreases fast for $|\mathbf{j}| \gg 1$.

The plane waves (or Fourier modes) on \mathbb{T}^2 are accordingly defined as $\phi_{\mathbf{k}}(\mathbf{x}) \stackrel{\text{def}}{=} \exp(2i\mathbf{x} \wedge \mathbf{k})$, for $\mathbf{k} \in \mathbb{Z}^2$. They are obviously the eigendensities of the coarse-graining operator:

$$D_\epsilon \phi_{\mathbf{k}} = \tilde{K}(\epsilon\mathbf{k}) \phi_{\mathbf{k}} \quad (6)$$

The fast decrease of the eigenvalues as $|\mathbf{k}| \gg 1$ implies that the operator D_ϵ is not only compact, but also trace-class. It kills the small-wave-length modes, effectively truncating the Fourier decomposition of $f(\mathbf{x})$ at a cutoff $|\mathbf{k}| \leq \frac{1}{\epsilon}$. For some instances, we will actually replace the smooth function $\tilde{K}(\mathbf{j})$ by a sharp cutoff $\chi_{\leq 1/\epsilon}(\mathbf{j})$ (with χ_{\leq} the Heaviside step function).

1.2.2 Classical coarse-grained propagator

The noisy dynamics of the map M is represented by the product of the deterministic evolution P_M with the diffusion operator:

$$P_M \circ D_\epsilon \stackrel{\text{def}}{=} \mathbb{P}_M :$$

It may be more natural to define the noisy dynamics as the more ‘symmetric’ form $D_\epsilon \circ P_M$, but both definitions lead to the same spectral structure. \mathbb{P}_M describes a Markov process defined by the deterministic map M followed by a random jump on a scale ϵ .

We now give some general properties of this operator, independent of the particular map M . Like the regularizing operator D_ε, P_M , maps distributions into smooth functions, and is *compact* and *trace-class* on any functional space containing $C^1(\mathbb{T}^2)$, with a *spectrum independent on the space*. Its eigenvalues λ_j, μ_j are inside the unit disk (only $\mu_0 = 1$ is exactly on the unit circle), they are of finite multiplicity and admit the origin as only accumulation point. The eigenvalue μ_0 has for unique eigenfunction ϕ_0 .

In the next section we investigate in more detail the behaviour of these eigenvalues in the limit of small noise, stressing the difference between chaotic vs. regular maps.

2 Spectral properties of classical coarse-grained propagator

We now give some more precisions on the spectrum of P_M , in the limit of small noise, and for different classes of maps M . We start with the most chaotic maps, namely the Anosov diffeomorphisms defined in Section 1.1.3, the exponential mixing of which was described in section 1.1.4. We will then turn to the opposite case of “regular” maps on \mathbb{T}^2 .

2.1 Anosov diffeomorphism

We use the same notations as in section 1.1.4 for M an Anosov map. It was proven in [7] that the spectrum of P_M , outside some neighbourhood of the origin converges to the resonance spectrum of P_M on the Banach space B .

More precisely, for M a smooth Anosov canonical diffeomorphism on \mathbb{T}^2 with foliations of Hölder regularity $C^{1+\alpha}$ ($0 < \alpha < 1$), one considers the “associated” Banach space $B = B_M$ defined in terms of a coefficient $\alpha < 1$, such that the essential radius of P on B has for upper bound $\alpha = \max(\alpha_u; \alpha_s)$. The authors then construct a “weak” norm $\|\cdot\|_{k_w}$ on $L(B)$, such that $\|kP - Pk_w\| \rightarrow 0$ as $\alpha \rightarrow 0$. As a consequence, for any $1 > r > \alpha$, any λ in the annulus $R_r = \{\lambda \mid |\lambda| = r\}$ and any $\varepsilon > 0$ small enough, the spectral projector \mathcal{P}_ε (resp. \mathcal{P}_ε) of P (resp. P) in the disk $\{z \mid |z| < r\}$ satisfy $\|\mathcal{P}_\varepsilon - \mathcal{P}_\varepsilon\|_{k_w} \rightarrow 0$. Both projectors therefore have the same rank for ε small enough, this rank being zero if the disk contains no resonance λ_j .

This proves that the spectrum of P in the annulus R_r converges (with multiplicity) to the set of resonances λ_j as $\alpha \rightarrow 0$, and the eigenmodes of P weakly converge to corresponding eigenmodes of P (since the latter are genuine distributions, the convergence can only hold in a weak sense).

Remarks:

These results also apply to the ‘symmetric’ coarse-graining $D_\varepsilon = P_\varepsilon D_\varepsilon$

It is reasonable to conjecture that these results hold as well if the coarse-graining kernel $K(x)$ is not compactly supported on \mathbb{R}^2 , but decreases sufficiently fast, for

instance if one takes the Gaussian $G(\mathbf{x}) \stackrel{\text{def}}{=} e^{-\mathbf{x}^2}$, $G(\cdot) = e^{-\mathbf{j}^2}$, as was done in [1, 22]. As a broader generalization, we will sometimes consider a coarse-graining defined by a sharp cut-off in Fourier space, $\mathcal{K}(\cdot) = (1 - \mathbf{j}^2)$, similar to the method used in [26].

If the map M and the kernel $K(\mathbf{x})$ are real-analytic, we conjecture that the spectrum of P on any ring R_r with $r > 0$ converges to the resonances in R_r (cf. the remark at the end of section 1.1.4).

The (discrete) spectrum of P is the same on any space S larger than C^1 , in particular on L^2 , and this is the space we will consider from now on (more precisely, its subspace \mathcal{L}_0^2). This spectrum drastically differs from the absolutely continuous unitary spectrum of the “pure” propagator P on that space (cf. section 1.1). The unitary spectrum is thus *unstable* upon the coarse-graining D : when switching on the noise, the spectral radius of P on \mathcal{L}_0^2 suddenly collapses from 1 to $\mathbf{j}_1 \mathbf{j} < 1$. As we will see in the next sections, this collapse is characteristic of chaotic maps. In the next section, explicitly describe this collapse for the case of the hyperbolic generalized cat maps.

2.1.1 Example of an Anosov map: the hyperbolic linear automorphisms

In this section we review [14, 21] the spectral analysis of the (pure vs. noisy) propagator when the map is a hyperbolic linear automorphism of \mathbb{T}^2 (cf. section 1.1.3). The map is given by a matrix $A \in \text{SL}(2; \mathbb{Z})$ with $|\text{tr} A| > 2$. The unitary operator P_A on \mathcal{L}_0^2 acts very simply on the basis of Fourier modes $\mathbf{k}, \mathbf{k} \in \mathbb{Z}^2 = \mathbb{Z}^2 \setminus \{0\}$, namely as a permutation:

$$P_A \mathbf{k}(\mathbf{x}) = \mathbf{k}(A^{-1}\mathbf{x}) = A\mathbf{k}(\mathbf{x}): \quad (7)$$

This evolution induces *orbits* on the Fourier lattice \mathbb{Z}^2 , which we will denote by $O(\mathbf{k}_0) = \{A^t \mathbf{k}_0; t \in \mathbb{Z}\}$. Due to the hyperbolicity of A , each orbit is infinite, so that the linear combinations of the modes $\mathbf{k} \in A^t \mathbf{k}_0; t \in \mathbb{Z}$ span an infinite-dimensional invariant subspace of \mathcal{L}_0^2 , which we call $\text{Span} O(\mathbf{k}_0)$. The spectral measure of P_A associated with this subspace is of Lebesgue type (as usual when the operator acts as a shift [33]). The number of distinct orbits being infinite, the spectrum of P_A on \mathcal{L}_0^2 is Lebesgue with infinite multiplicity.

Now we consider the coarse-grained propagator $P_{\mathcal{A}} = D \circ P_A$. Since the \mathbf{k} are eigenfunctions of D (cf. Eq. (6)), $P_{\mathcal{A}}$ will also act as a permutation inside each orbit $O(\mathbf{k}_0)$, but now at each step the mode \mathbf{k} is multiplied by $\mathcal{K}(\mathbf{k})$. Therefore, the operator $P_{\mathcal{A}}$ restricted to the invariant subspace $\text{Span} O(\mathbf{k}_0)$ can be represented as follows (the notation $(\cdot; \cdot)$ denotes the scalar product on \mathcal{L}_0^2):

$$P_{\mathcal{A}} \mathcal{D}(\mathbf{k}_0) = \sum_{t \in \mathbb{Z}} \mathcal{K}(A^{t+1} \mathbf{k}_0) (A^t \mathbf{k}_0; \cdot) A^{t+1} \mathbf{k}_0: \quad (8)$$

Since $\mathcal{K}(A^t \mathbf{k}_0) \rightarrow 0$ for $t \rightarrow \pm \infty$, the factors $\mathcal{K}(A^{t+1} \mathbf{k}_0)$ vanish in both limits. As a result, the spectrum of $P_{\mathcal{A}} \mathcal{D}(\mathbf{k}_0)$ reduces to the single point $\mathbf{f}0\mathbf{g}$ (it is not an eigenvalue, but

essential spectrum) [33]. Taking all the orbits $\mathcal{O}(\mathbf{k}_0)$ into account, the spectrum of $\mathbb{P}_{\mathcal{A}}$ on \mathcal{L}^2_0 is still reduced to the singleton $\{0\}$. By taking all orbits into account, the spectrum of $\mathbb{P}_{\mathcal{A}}$ on \mathcal{L}^2_0 also reduces to $\{0\}$: for linear hyperbolic maps, the collapse of the Lebesgue unitary spectrum through coarse-graining is ‘maximal’.

2.2 Coarse-graining of regular dynamics

In the previous sections we have considered classical propagators of Anosov diffeomorphisms on \mathbb{T}^2 . We now describe the opposite case of an *integrable* map on \mathbb{T}^2 . The notion of integrability for a map is not so clear as for a Hamiltonian flow. In view of the examples below, the definition should include the stroboscopic map $\mathbb{M}_H = \tau_{\frac{1}{H}}$ of the flow generated by an autonomous Hamiltonian $H(\mathbf{x})$ on \mathbb{T}^2 , but it should also encompass elliptic and parabolic automorphisms, as well as rational translations. A required property is that the phase space \mathbb{T}^2 splits into a union of invariant 1-dimensional (not necessarily connected) closed submanifolds with possible singularity points (cf. the zero-energy set for the Harper Hamiltonian). A more or less equivalent condition to integrability is that the map leaves invariant a nowhere constant smooth function $H(\mathbf{x})$, the level curves of which provide the above submanifolds. As a result, any density $\rho(\mathbf{x}) = f(H(\mathbf{x}))$ is invariant through \mathbb{P}_M as well, so that \mathbb{P}_M has an infinite-dimensional eigenspace of invariant densities on \mathcal{L}^2_0 (which we will call V_{inv}).

The rest of the spectrum of \mathbb{P}_M can be of various types, as we will see (it can be pure point or absolutely continuous, be a mixture, etc.). For this reason, a general statement concerning the coarse-grained spectrum of these maps cannot be very precise.

In the following sections we consider some simple examples of integrable maps for which (part of) the spectrum can be analyzed in detail. We then discuss (mostly by handwaving) the general case of integrable maps.

2.2.1 Translations on the torus

The simplest nontrivial maps on \mathbb{T}^2 are the translations $\mathbf{x} \mapsto \mathbb{T}_v \mathbf{x} = \mathbf{x} + v \pmod{\mathbb{T}^2}$, which do not derive from a Hamiltonian on the torus. A translation is either ergodic (yet non-mixing) or integrable (see below).

The spectrum of the corresponding Perron-Frobenius operator $\mathbb{P}_v = \mathbb{P}_{\mathbb{T}_v}$ on \mathcal{L}^2_0 is easy to describe [14]: \mathbb{P}_v admits the Fourier modes $\phi_{\mathbf{k}}$ as eigenstates, with eigenvalues $e^{2i\mathbf{k} \cdot v}$. The spectrum of \mathbb{P}_v is therefore pure point, with possible degeneracies. The spectrum of the coarse-grained propagator $\mathbb{P}_{\mathcal{A}} = \mathbb{D} \circ \mathbb{P}_v$ on \mathcal{L}^2_0 is also easy to describe: each Fourier mode $\phi_{\mathbf{k}}$ is an eigenfunction with eigenvalue $\mathcal{K}(\mathbf{k}) e^{2i\mathbf{k} \cdot v}$ inside the unit disk. From the small- ϵ expansion $\mathcal{K}(\mathbf{k}) = 1 - \epsilon^2 Q(\mathbf{k})$, the eigenvalues corresponding to long wavelengths ($|\mathbf{k}| \ll 1$) are close to the unit circle for small ϵ , while the short wavelength eigenvalues ($|\mathbf{k}| \gg 1$) accumulate near the origin. We now describe how the global aspect of the spectrum qualitatively depends on the translation vector v .

\mathbb{T}_v is ergodic iff the coefficients v_1, v_2 as well as their ratio $\frac{v_1}{v_2}$ are irrational: in that case, the equation $\mathbf{k} \cdot v \in \mathbb{Z}$ has no solution for $\mathbf{k} \in \mathbb{Z}^2$. The spectrum of \mathbb{P}_v forms a

dense subgroup of the unit circle, all eigenvalues being simple. In the limit $\epsilon \rightarrow 0$, the spectrum of P_ν becomes “dense” in the unit disk (a similar quantum spectrum is plotted on Fig. 4, right).

If one of the coefficients ν_1, ν_2 is rational, T_ν leaves invariant a family of parallel 1-dimensional “affine” submanifolds, and is therefore integrable. For instance, if we take $\nu_1 = \frac{r}{s}$ (with r, s coprime integers) and ν_2 irrational, then for any $\alpha \in [0, 1]$, the union of vertical lines $\sum_{l=0}^{s-1} \alpha = \alpha + \frac{l}{s}$ is invariant (if $s > 1$, this set is nonconnected). The spectrum of P_ν is still dense on the circle, but all eigenvalues are now infinitely degenerate: for any k_0 , the modes $k = k_0 + (0; js)$, $j \in \mathbb{Z}$ share the eigenvalue $e^{2i k_0 \wedge \nu}$. The eigenvalues of P_ν are at most finitely-degenerate: to each phase $e^{2i k_0 \wedge \nu}$ corresponds a “string” of eigenvalues of decreasing moduli, the largest one being at a distance ϵ^2 from the unit circle. As in the previous case, the spectrum densely fills the unit disk as $\epsilon \rightarrow 0$.

If both ν_1, ν_2 are rational of the form $\frac{r_1}{s}; \frac{r_2}{s}$ with $\gcd(r_1; r_2; s) = 1$, each point of T^2 is periodic with period s , the map is integrable. The only eigenvalues of P_ν are of the phases $e^{2i j \wedge s}$, all being infinitely degenerate. The eigenvalues of P_ν are at most finitely degenerate, they are grouped into s strings of phases $e^{2i j \wedge s}$, $j = 0; \dots; s-1$. For small ϵ , the eigenvalues become dense along these strings, the largest eigenvalue at a distance ϵ^2 from the unit circle (this spectrum is similar with the quantum one plotted on Fig. 4, left).

Comparing the first and second case, we see that the spectrum of P cannot unambiguously differentiate an ergodic from an integrable map: both may have eigenvalues close to the unit circle. On the other hand, the second and third cases both correspond to integrable maps. Yet, their small-noise spectra look quite different from one another.

2.2.2 Non-hyperbolic linear automorphisms of the torus

Another class of non-mixing linear maps on T^2 is provided by the non-hyperbolic linear automorphisms. These automorphisms split into two classes (for notations, we refer to section 2.1.1):

the elliptic transformations ($|\text{tr} A| < 2$), like for instance the $\epsilon=2$ -rotation given by the matrix $J = \begin{pmatrix} 0 & 1 \\ 1 & 0 \end{pmatrix}$. As opposed to the hyperbolic case, each Fourier orbit $O(k_0) = \{J^j k_0; j = 0; \dots; 3g\}$ is finite of period 4, and $\text{Span} O(k_0)$ splits into 4 eigenspaces associated with the eigenvalues $\pm i; \pm 1 = 0; \dots; 3g$. Switching on coarse-graining, the eigenvalues now read $\epsilon^{\pm j} k_0$, with $k_0 = \frac{1}{4} \mathcal{K}(\epsilon) \mathcal{K}(\epsilon J k_0)$. The spectrum of P_ν on T^2 therefore consists in four strings along the four half-axes, which become dense in the limit $\epsilon \rightarrow 0$ (see fig. 1 for the analogous quantum spectrum). Similarly, an elliptic transformation of trace $\text{tr} A = 1$ will satisfy $A^6 = 1$, therefore

the spectrum of $P_{\mathcal{A}}$ forms 6 strings. An elliptic transformation of $\text{tr}A = 1$ will lead to 3 strings.

the parabolic transformations (or parabolic shears), given by matrices of the type $S = \begin{pmatrix} 1 & s \\ 0 & 1 \end{pmatrix}$, $s \in \mathbb{Z}$. The dynamics reads $(q; p) \mapsto (q + sp; p)$, so any periodic function of the momentum p is a conserved quantity. The Fourier vector $k_0 = (k_1; k_2)$ generates the orbit $O(k_0) = \{fk_0 + (jsk_2; 0); j \in \mathbb{Z}\}$: if $k_2 = 0$ (meaning that k does not depend on q), the mode δ_{k_0} is invariant and the orbit is a singleton; on the opposite, if $k_2 \neq 0$, $O(k_0)$ is infinite, and leads to Lebesgue spectrum for $P_{S \mathcal{D}(k_0)}$. The full spectrum of P_S on \mathcal{L}^2_0 is therefore the union of the infinitely degenerate eigenvalue 1 with a countable Lebesgue spectrum [14]. In the case $k_2 \neq 0$, the noisy propagator $P_{\mathcal{S}}$ acts on $\text{Span}O(k_0)$ as in Eq. (8), upon replacing A by S . Since the wavevectors $\mathcal{B}^{\pm}k_0$ diverge in both limits $\tau \rightarrow 1$, the associated spectrum reduces to the singleton $\{0\}$. On the opposite, each mode $\delta_{(l;0)}$ is eigenstate of $P_{\mathcal{S}}$ with eigenvalue $\mathcal{K}(l;0)$: these modes form a string along the real axis, which becomes dense as $\tau \rightarrow 0$.

2.2.3 Nonlinear shear

If we perturb the linear parabolic shear S (cf. last section) with the stroboscopic map of the flow generated by a Hamiltonian of the form $F(p)$, we obtain a nonlinear shear $(q; p) \mapsto (q + sp + F^0(p); p)$. We assume that $s > 0$, and that the Hamiltonian F satisfies $s + F^0(p) > 0$ everywhere. This map still conserves momentum, so that any density $\rho(p)$ is invariant. Among these, the Fourier modes $\delta_{(l;0)}$ are eigenstates of P , with eigenvalues $\mathcal{K}(l;0)$: they form the same string of real eigenvalues as for the linear shear.

For any $n \in \mathbb{Z}$, P and P^n leave invariant the subspace $V_n = \text{Span} \{e^{2i n q}(p); p \in L^2(\mathbb{S}^1)\}$, and their spectra on this subspace can be partially described, at least if one takes F^0 small enough and replaces the kernel $\mathcal{K}(\cdot)$ by the cutoff $(1 - \frac{|\cdot|}{n})^2$ (such that D projects to a finite-dimensional subspace). The spectrum of P on V_n is absolutely continuous, while that of P^n is contained in a small neighbourhood of the origin, uniformly with respect to n and τ (see Appendix A.1 for details). The spectrum should be qualitatively the same if $\mathcal{K}(\cdot)$ is only of fast decrease at infinity.

2.2.4 Stroboscopic map of the Harper Hamiltonian flow

As a last example of integrable map, we consider the Harper Hamiltonian on the torus

$$H(x) = \cos(q) + \cos(p) = \frac{1}{2} (\delta_{(1;0)} + \delta_{(-1;0)} + \delta_{(0;1)} + \delta_{(0;-1)});$$

and take its stroboscopic map $M = \tau^{\frac{1}{H}}$. The invariant densities are of the form $\rho(x) = f(H(x))$. As opposed to what happened for the parabolic shear, V_{inv} is not invariant through the diffusion operator D , so the spectrum of P is more complicated to analyze.

Still, if we take a coarse-graining kernel satisfying $\mathcal{K}(\mathbf{x}) = \mathcal{K}(j_1 j_2)$ along the axes of slopes $(0; 1=2; 1; 2; 1)$ then the invariant functions $H(\mathbf{x})$, $(H(\mathbf{x}))^2$ and $(H(\mathbf{x}))^3$ are eigenstates of D and therefore of P , with respective eigenvalues $\mathcal{K}(1)$, $\mathcal{K}(2)$ and $\mathcal{K}(3)$ (if the kernel only satisfies $\mathcal{K}((0; \mathbf{x})) = \mathcal{K}((\mathbf{x}; 0))$ together with even parity, then $H(\mathbf{x})$ will be eigenstate of P with eigenvalue $\mathcal{K}((\mathbf{x}; 0))$). These eigenvalues are real and approach unity as $\epsilon \rightarrow 0$. Numerically, they are the three first elements (resp. the first element) of a string of real eigenvalues connecting unity to the origin, the further elements of the string being mixtures of invariant and non-invariant densities (see Fig. 5, right for a similar quantum spectrum).

2.2.5 General behaviour for an integrable map

After these examples, we want to describe the spectrum of P_M ; for M an integrable map, say the stroboscopic map of an autonomous Hamiltonian H . As we already explained, the space V_{inv} of invariant densities is infinite-dimensional, containing (at least) all densities $f(H(\mathbf{x}))$. When applying the coarse-graining D , one in general mixes these invariant densities with non-invariant ones (as opposed to what happened for the linear maps described above). Using ideas of degenerate perturbation theory, we conjecture the following behaviour, which is supported by numerical investigations [26, 22].

The invariant subspace V_{inv} contains modes ρ_{lw} with long-wavelength fluctuations (that is, densities for which the Fourier spectrum is concentrated in a finite region near $k = 0$). For ϵ small, these modes are hardly modified by the coarse-graining operator: $D \rho_{\text{lw}} = \rho_{\text{lw}} + O(\epsilon^2)$. This suggests that P has an eigenstate of the type $\rho_{\text{lw}} + O(\epsilon^2)$, of eigenvalue $1 + O(\epsilon^2)$. On the other hand, V_{inv} also contains highly fluctuating modes, which will be very damped by D , and should lead to eigenstates of P close to the origin. As a whole, the hybridation of V_{inv} leads to a string of modes connecting unity to the origin.

Conclusion: qualitatively different spectra

We have exhibited a *qualitative difference* of the coarse-grained Perron-Frobenius spectra between, on one side, the chaotic maps (Anosov), on the other side, non-mixing maps, including ergodic translations and integrable maps.

In the latter case, the spectrum of P on the subspace $\mathcal{L}_0^2(\mathbb{T}^2)$ of $L^2(\mathbb{T}^2)$ comes close to the unit circle for small ϵ , either along 1-dimensional strings “connecting” the origin to infinitely degenerate eigenvalues of P (among which unity), or by densely filling the unit disk (for ergodic translations). A common feature is that any annulus $r < |z| < 1$ (or any open neighbourhood of unity) contains more and more eigenvalues of P in the small-noise limit $\epsilon \rightarrow 0$.

On the opposite, for an Anosov map the spectrum of P on \mathcal{L}_0^2 is contained inside a disk of radius $R < 1$, uniformly for small enough ϵ . This spectrum consists in a finite number (possibly zero) of finitely degenerate eigenvalues (asymptotically close to the Ruelle resonances) inside an annulus $r < |z| < R$, the remaining eigenvalues having moduli smaller than r .

The numerical results of [26, 22] go beyond this statement: the authors consider maps with mixed dynamics (repectively the kicked top on the sphere, and the standard map or kicked rotor on the cylinder), that is systems for which the phase space splits into “regular islands” embedded in a “chaotic sea”. They study the spectrum of the coarse-grained Perron-Frobenius operator (the coarse-graining is taken as a cut-off in Fourier space), and showed the presence of eigenvalues close to the unit circle, whose eigendensities are supported on the regular islands; on the other hand, they also find some eigenvalues inside the unit circle, which are associated with the chaotic part of phase space, and therefore interpreted as generalized Ruelle resonances. The existence of such resonances seems difficult to prove mathematically, since the systems are far from being uniformly hyperbolic.

3 Quantum coarse-grained evolution

After studying the effect of noise on classical propagators, we now turn to noisy quantum maps, obtained by quantizing the classical ones. Although we restrict below to maps on \mathbb{T}^2 , the main result of this section (Theorem 1) may be straightforwardly generalized to quantum maps on any compact phase space (provided one properly adapts the definition of the coarse-graining operator). We start the section by recalling the framework of quantized maps on the 2-torus.

3.1 Quantum propagator on the torus

3.1.1 Quantum Hilbert space and observables

We shortly review the construction of quantum mechanics on \mathbb{T}^2 , in order to fix notations. For any value of $\hbar > 0$, the Weyl-Heisenberg group associates to each vector $\mathbf{v} = (v_1; v_2) \in \mathbb{R}^2$ the “quantum translation” $\hat{T}_{\mathbf{v}} = \exp \frac{i}{\hbar} (v_2 \hat{q} - v_1 \hat{p})$ which acts unitarily on $L^2(\mathbb{R})$. These translations satisfy the relations $\hat{T}_{\mathbf{v}} \hat{T}_{\mathbf{v}^0} = e^{i \mathbf{v} \wedge \mathbf{v}^0} \hat{T}_{\mathbf{v} + \mathbf{v}^0}$.

The “torus wavefunctions” are then defined as distributions $\mathfrak{f}_{\mathbf{j}} \in \mathcal{S}'(\mathbb{R})$ satisfying the biperiodicity conditions $\hat{T}_{(0;1)} \mathfrak{f}_{\mathbf{j}} = \mathfrak{f}_{\mathbf{j} + \mathbf{i}}$ and $\hat{T}_{(1;0)} \mathfrak{f}_{\mathbf{j}} = \mathfrak{f}_{\mathbf{j} + \mathbf{i}}$. Due to the group relations, such distributions exist iff \hbar satisfies the condition $(2/\hbar) \in \mathbb{Z}$ (such a value for \hbar will be called *admissible*). They then form a space of dimension N , which will be noted H_N [18]. A basis of this space is provided by the “Dirac combs” $\mathfrak{f}_{\mathbf{j}} \in H_N$ $\mathfrak{g}_{\mathbf{j} = 0; \dots; N-1}$ defined as:

$$\mathfrak{f}_{\mathbf{j}} = \sum_{z \in \mathbb{Z}} \delta(\mathbf{q} - \mathbf{q} + \mathbf{j}); \quad \text{with } \mathbf{q} = \frac{\mathbf{j}}{N}; \quad (9)$$

By construction, $\mathfrak{f}_{\mathbf{j} + N \mathbf{i}} = \mathfrak{f}_{\mathbf{j}}$, so the index \mathbf{j} must be understood modulo N . For practical reasons, we will choose the following representatives of integers modulo N : $Z_N = \{ \frac{N}{2} + 1; \dots; \frac{N}{2} \}$ for N even, $Z_N = \{ \frac{N-1}{2} + 1; \dots; \frac{N-1}{2} \}$ for N odd.

The quantum translation $\hat{T}_{\mathbf{v}}$ acts inside H_N iff \mathbf{v} is on the square lattice of side $1/N$, that is $\mathbf{v} = \frac{V_1}{N}; \frac{V_2}{N}$ with $V_i \in \mathbb{Z}$. Besides, each translation with integer coefficients acts on

\mathbb{H}_N as a multiple of the identity. As a result, the set $\{\hat{T}_{v \Rightarrow N}^{\circ}; v \in \mathbb{Z}_N^2\}$ forms a basis of the space of linear operators $\mathcal{L}(\mathbb{H}_N)$. This basis can be used to define the Weyl quantization of smooth observables $f \in C^1(\mathbb{T}^2)$. From the Fourier decomposition $f = \sum_{k \in \mathbb{Z}^2} \hat{f}(k) e^{i k \cdot x}$, the Weyl quantization of the observable f is defined as

$$\hat{f} = \mathcal{O}_{\mathbb{P}_N}(f) \stackrel{\text{def}}{=} \sum_{k \in \mathbb{Z}^2} \hat{f}(k) \hat{T}_{k \Rightarrow N} = \sum_{k \in \mathbb{Z}_N^2} \hat{T}_{k \Rightarrow N} \sum_{\ell \in \mathbb{Z}^2} (1)^{N \cdot (1/2 + k) \cdot \ell} \hat{f}(k + N \ell) : \quad (10)$$

The ‘‘converse’’ of Weyl quantization, that is the **Weyl symbol** (or Wigner function) $W_{\hat{B}}(\mathbf{x})$ of an operator $\hat{B} \in \mathcal{L}(\mathbb{H}_N)$ is also easily defined through its Fourier transform: for each $k \in \mathbb{Z}^2$, its Fourier coefficient $\tilde{W}_{\hat{B}}(k)$ is given by $\tilde{W}_{\hat{B}}(k) = \frac{1}{N} \text{tr} \hat{T}_{k \Rightarrow N}^y \hat{B}$. These Fourier coefficients are N -periodic (up to a sign), so that the ‘‘function’’ $W_{\hat{B}}(\mathbf{x})$ is a periodic combination of Dirac peaks on the lattice of side $1=2N$ [18]. Alternatively, a **polynomial Weyl symbol** was defined in [15] as the finite sum

$$W_{\hat{B}}^{\text{P}}(\mathbf{x}) = \sum_{k \in \mathbb{Z}_N^2} \tilde{W}_{\hat{B}}(k) e^{2i \mathbf{x} \cdot k} :$$

As opposed to the former symbol, the polynomial symbol depends on the specific choice for the representative \mathbb{Z}_N (the choice we made, with maximum symmetry around the origin, seems more natural in this respect). The polynomial symbol map together with $\mathcal{O}_{\mathbb{P}_N}$ yield an *isometric isomorphism* between the subspace $\mathcal{I}_N \stackrel{\text{def}}{=} \text{Span} \{f_k; k \in \mathbb{Z}_N^2\}$ of $\mathcal{L}^2(\mathbb{T}^2)$ and the space of observables on \mathbb{H}_N equipped with the Hilbert-Schmidt scalar product $(\hat{B}; \hat{C}) = \frac{1}{N} \text{tr}(\hat{B}^y \hat{C})$. Since the Hilbert-Schmidt norm differs from the usual operator norm on $\mathcal{L}(\mathbb{H}_N)$, we will denote by \mathcal{L}_N^2 the space of observables on \mathbb{H}_N (that is, $N \times N$ matrices) equipped with the Hilbert-Schmidt norm.

3.1.2 Quantization of canonical maps

We now briefly explain how to quantize a canonical map M on \mathbb{T}^2 . The aim is to define for each $N \in \mathbb{N}$ a unitary operator on \mathbb{H}_N (which we will denote by \hat{M}_N or simply \hat{M}) which satisfies prescribed semiclassical properties [36]. These properties do not unambiguously define the sequence of unitary matrices, so a choice has to be made (in [38], a Toeplitz quantization is proposed for symplectic maps on Kähler manifolds). We present here another quantization prescription, which uses the following decomposition of any canonical map M on \mathbb{T}^2 [12]:

$$M = A \circ T_v \circ \tau_H^1 : \quad (11)$$

In this formula, the linear automorphism $A \in \text{SL}(2; \mathbb{Z})$ and the translation T_v are uniquely defined. On the opposite, the last factor correspond to the stroboscopic map of the flow of a time-dependent periodic Hamiltonian $H \in C^1(\mathbb{T}^2 \times \mathbb{T})$; this Hamiltonian is not unique[0,1], since two Hamiltonians $H_1 \in \mathcal{H}_2$ may lead to the same stroboscopic map $\tau_{H_1}^1 = \tau_{H_2}^1$. From this decomposition, one can quantize M as follows [20]. First, one quantizes *à la* Weyl the

Hamiltonian $H(\mathbf{t})$ into the operator $\hat{H}(\mathbf{t})$, then take for the quantization of $\rho_{\mathcal{H}}^{-1}$ the time-ordered exponential $T e^{i \int_0^{\mathbf{t}} dt \hat{H}(\mathbf{t})}$. Second, one may quantize the translation $T_{\mathbf{v}}$ with the quantum translation $\hat{T}_{\mathbf{v}^{(N)}}$, where the vector $\mathbf{v}^{(N)}$ belongs to the $1=N$ -lattice and is close to \mathbf{v} , for instance take $\mathbf{v}^{(N)} = \frac{(N \mathbf{v}_1; N \mathbf{v}_2)}{N}$ [27]. Third, provided A satisfies the condition $A \equiv \text{Id} \pmod{2}$ or $A \equiv x \pmod{2}$, the linear automorphism A is “naturally” quantized into a unitary matrix \hat{A}_N [18] (this condition may be relaxed if one generalizes the quantum Hilbert space \mathcal{H}_N to arbitrary “Bloch angles” [10]). Finally, the map M is quantized on \mathcal{H}_N as the $N \times N$ unitary matrix:

$$\hat{M}_N = \hat{A}_N \hat{T}_{\mathbf{v}^{(N)}} T e^{i \int_0^{\mathbf{t}} dt \hat{H}(\mathbf{t})} : \quad (12)$$

This choice for the quantum map automatically satisfies the prescribed semiclassical properties, in particular it satisfies the Egorov property [10, 27]: for any classical observable $\mathcal{O} \in C^1(\mathbb{T}^2)$,

$$\hat{M}_N \circ \mathcal{P}_N(\mathcal{O}) \hat{M}_N^{-1} \circ \mathcal{P}_N(\mathcal{O})^{-1} = \mathcal{O} + \mathcal{O}^{(N)} + o(1) : \quad (13)$$

This means that the quantization and finite-time evolution of densities commute in the semiclassical limit (the convergence holds for the operator norm in $L(\mathcal{H}_N)$).

In practice, the classical maps we consider are all defined as products of automorphisms, translations and Hamiltonian maps, so they admit a “natural” quantization.

3.1.3 Propagator of quantum densities

The quantum map \hat{M} propagates quantum states $\rho \in \mathcal{H}_N$. A density matrix $\hat{\rho}$ is an element of the space $L_N^2 = \mathcal{H}_N \otimes \mathcal{H}_N$, and its evolution through the quantum map reads $\hat{\rho} \mapsto \hat{M} \hat{\rho} \hat{M}^{-1} = \text{ad}(\hat{M}) \hat{\rho}$. The operator $\hat{P}_M \stackrel{\text{def}}{=} \text{ad}(\hat{M})$ acting on the space L_N^2 is the quantum analogue of the Perron-Frobenius operator \mathcal{P}_M acting on classical densities. \hat{P}_M is unitary, with eigenvalues $f e^{i \langle \mathbf{j}, \mathbf{i} \rangle}$; $\mathbf{i}, \mathbf{j} = 1, \dots, N$, where $f e^{i \langle \mathbf{j}, \mathbf{i} \rangle}$ are the eigenvalues of the matrix \hat{M} . As a contrast with its classical analogue, the space of invariant densities through \hat{P}_M is at least N -dimensional, since it contains all the rank-1 projectors $|\mathbf{j}\rangle\langle\mathbf{i}|$ where $|\mathbf{i}\rangle$ are the eigenstates of \hat{M} .

The operator \hat{P} acting on densities is called a *superoperator* in the theory of measurement, to contrast with an operator acting on \mathcal{H}_N . Being the adjoint action of a unitary matrix, it conserves the *purity* of the density, which means that a pure density $\hat{\rho} = |\mathbf{j}\rangle\langle\mathbf{j}|$ is mapped onto a pure density $\hat{P} \hat{\rho} = |\mathbf{j}'\rangle\langle\mathbf{j}'|$. We notice that \hat{P} conserves the *trace* of the density, that is the quantum counterpart of the total probability of the density.

3.2 Quantum coarse-graining operator

As we noticed above, the spectrum of \hat{P} on L_N^2 is qualitatively different from that of \mathcal{P} on $L^2(\mathbb{T}^2)$: the former has at least N invariant eigenstates, while the latter may have only one if M is ergodic. In the classical framework, we explained how the spectrum of \mathcal{P} was sensitive to the functional space on which \mathcal{P} was applied. This is not any more

the case in the quantum framework, since the propagator is a finite-dimensional matrix. However, we showed in section 2 an alternative way to obtain the (nonunitary) resonance spectrum of an Anosov map, namely by introducing some noise and studying the spectrum of the noisy propagator $\mathbb{P} = \mathbb{D} \circ \mathbb{P}$ on the space $\mathbb{L}^2(\mathbb{T}^2)$. This procedure can also be carried out at the quantum level, by first defining a “quantum coarse-graining” or “quantum diffusion” (super)operator $\hat{\mathbb{D}}$, and a coarse-grained quantum propagator $\hat{\mathbb{P}}$, then studying its spectrum on $\mathbb{L}^2_{\mathbb{N}}$. The connection between classical and quantum frameworks will require to take the semiclassical limit $\mathbb{N} \rightarrow 1$.

3.2.1 Definition

We define the coarse-graining superoperator by analogy with the classical one (5). The latter can be expressed as follows:

$$\text{Tr} \int_{\mathbb{T}^2} \mathbb{D} f(\mathbf{x}) = \int_{\mathbb{T}^2} d\mathbf{v} K(\mathbf{v})(\mathbf{x} - \mathbf{v}) = \int_{\mathbb{T}^2} d\mathbf{v} K(\mathbf{v}) (\mathbb{P}_{\mathbf{v}}^{-1}) (\mathbf{x}); \quad (14)$$

where $\mathbb{P}_{\mathbf{v}}$ is the Perron-Frobenius operator for the translation $\mathbb{T}_{\mathbf{v}}$. Since $\mathbb{T}_{\mathbf{v}}$ is quantized into the unitary matrix $\hat{\mathbb{T}}_{\mathbf{v}(\mathbb{N})}$, a natural way to define a quantum coarse-graining superoperator would be the integral

$$\int_{\mathbb{T}^2} d\mathbf{v} K(\mathbf{v}) \hat{\mathbb{P}}_{\mathbf{v}(\mathbb{N})} :$$

For convenience, we prefer a slightly different definition. The map $\mathbf{v} \mapsto \mathbf{v}(\mathbb{N})$ is constant on squares of side $1/\mathbb{N}$, so the above integral reduces to a finite sum over $\mathbb{V} \subset \mathbb{Z}_{\mathbb{N}}^2$, with each operator $\hat{\mathbb{P}}_{\mathbf{v}(\mathbb{N})}$ multiplied by the average of K over the corresponding square. K being a smooth function, this average is semiclassically equal to the value $K(\mathbf{v}(\mathbb{N}))$, therefore for \mathbb{N} large the above integral is well approximated by the sum:

$$\hat{\mathbb{D}} = \frac{F(\cdot; \mathbb{N})}{\mathbb{N}^2} \sum_{\mathbf{v} \in \mathbb{Z}_{\mathbb{N}}^2} K(\mathbf{v}(\mathbb{N})) \text{ad } \hat{\mathbb{T}}_{\mathbf{v}(\mathbb{N})} : \quad (15)$$

The prefactor $F(\cdot; \mathbb{N})$ guarantees that $\hat{\mathbb{D}}$ conserves the trace, that is $\hat{\mathbb{D}} \hat{\rho}_0 = \hat{\rho}_0$. This factor is easily expressed in terms of the 2-dimensional Jacobi theta function:

$$F(\cdot; \mathbb{N}) \stackrel{\text{def}}{=} \sum_{\mathbf{z} \in \mathbb{Z}^2} \mathcal{K}(\mathbf{N}(\cdot + \mathbf{z})); \quad \mathbf{z} \in \mathbb{Z}^2: \quad (16)$$

For Gaussian coarse-graining $K(\mathbf{x}) = G(\mathbf{x}) = e^{-\mathbf{x}^2}$, this function reduces to the product of two classical one-dimensional theta functions. In the limit $\mathbb{N} \rightarrow 1$, the function \mathcal{K} is peaked around the point $\mathbf{x} = 0$, due to the fast decrease of $\mathcal{K}(\cdot)$. Now, one easily checks that $F(\cdot; \mathbb{N}) = \mathcal{K}(\mathbf{N}; 0)^{-1}$ goes to $\mathcal{K}(0) = 1$ in the limit $\mathbb{N} \rightarrow 1$.

3.2.2 Spectrum of the quantum coarse-graining operator

The spectrum of \hat{D} on L_N^2 is as easy to analyze as that of D (see Eq. (6)). Using the group relation

$$\text{ad}(\hat{T}_v)\hat{T}_{v^0} = e^{i\frac{v \wedge v^0}{v}} \hat{T}_{v^0}; \quad (17)$$

we see that for any $k \in \mathbb{Z}_N^2$, the quantum translation $\hat{T}_{k=N}$ ($= O_{\mathbb{P}^N}(k)$) is eigenstate of \hat{D} with eigenvalue

$$d_{jk}^{(N)} = \frac{F(k; N)}{N^2} \sum_{v \in \mathbb{Z}_N^2} \mathcal{K}(v=N) e^{2i k \wedge \frac{v}{N}} = \frac{\mathcal{K}(N; k=N)}{\mathcal{K}(N; 0)}; \quad (18)$$

For fixed k and $N \gg 1$, one has the asymptotics $d_{jk}^{(N)} = \mathcal{K}(k) + O((N)^{-\alpha})$ for any power $\alpha > 0$, so that the quantum eigenvalue of $\hat{T}_{k=N}$ converges to the classical eigenvalue of \mathcal{K} . The estimate is sharper in the Gaussian case:

$$d_{jk}^{(N)} = e^{-2k^2} + O(e^{-\frac{(N)^2}{4}}); \quad (19)$$

so that the relative deviations between classical and quantum eigenvalues are exponentially small, uniformly on the modes $k \in \mathbb{Z}_N^2$ ($N \gg 1$) (with $\alpha > 0$ fixed). For the Gaussian case, both classical and quantum spectra are strictly positive, which is not true in general. The spectrum of \hat{D} for a Gaussian noise is plotted in Fig. 1.

If we replace $\mathcal{K}(k)$ by the sharp cutoff $\mathbb{1}_{|k| < 1}$; then $d_{jk}^{(N)} = 1$ for $|k| < 1$, $d_{jk}^{(N)} = 0$ otherwise: the coarse-graining truncates the expansion (10), keeping only short wavevectors (modulo \mathbb{Z}_N^2). In other words, \hat{D} truncates the Fourier series of the polynomial Weyl symbol $\bar{w}^{\mathbb{P}}$, keeping only the coefficients $|k| < 1$.

A Fourier cutoff was also used as definition of quantum coarse-graining in [26], but there the cutoff was applied to the **Husimi function** of $\hat{\rho}$.

3.2.3 Probabilistic interpretation and generalizations of coarse-graining

In a different physical framework (one-dimensional quantum spin chains), Prosen recently defined a similar quantum coarse-graining by truncating the densities onto finite-dimensional spaces [32]. In this case, the quantum densities are decomposed into sums of spin operators acting on finite sequences of spins (e.g. $\sigma_1(x) \sigma_1(x+1) \dots \sigma_1(x+1)$). The truncation consists in keeping only those operators for which $|k| < 1$.

The RHS of Eq. (15) expresses the superoperator \hat{D} in the *Kraus representation*, that is as a sum $\sum_j \text{ad}(\hat{E}_j)$, where the operators \hat{E}_j on H_N satisfy the trace-preserving condition $\sum_j \hat{E}_j^\dagger \hat{E}_j = \text{Id}_N$. Kraus superoperators conserve the trace and the ‘‘complete positivity’’ of density matrices [13].

The RHS of Eqs. (14,15) may be interpreted as a *random global jump* for the density, which jumps at a distance v with a probability $1/K(v)$. D and its quantum counterpart represent the average over all these random jumps. Since D or \hat{D} do not depend on

time, they therefore represent the classical and quantum versions of a memoryless Markov process.

In a different scope, a superoperator similar to \hat{D} was used in [28] to study the spectral correlations of the quantum map \hat{M} in the semiclassical limit. Coarse-graining was there interpreted as an averaging over a set of maps close to identity. The phase space was an arbitrary (quantizable) symplectic manifold, and the classical and quantum averagings were generated by a finite set of Hamiltonians $\{H_j\}_{j=1;\dots;f}$ and K a smooth probability kernel in f variables with compact support of scale ϵ around the origin. The classical and quantum coarse-graining operators are defined as:

$$\begin{aligned} D^{\{H_j\}}(\mathbf{x}) &= \int_{\mathbb{Z}^R} d^f t K(t) \prod_{j=1}^f e^{i t_j H_j}(\mathbf{x}) \\ \hat{D}^{\{H_j\}} &= \int_{\mathbb{R}^f} d^f t K(t) \text{ad} e^{i \sum_j t_j \hat{H}_j} \end{aligned} \quad (20)$$

This scheme is more general than what we have done on the torus: one does not need any group action on the phase space, but only a sufficient number of Hamiltonians. We recover our previous definition on the torus choosing for ‘‘Hamiltonians’’ the multivalued functions $H_1 = p \bmod 1$, $H_2 = q \bmod 1$ (these functions are not well-defined on \mathbb{T}^2 , but their flows are).

The qualitative spectral features of the classical coarse-grained propagator $D^{\{H_j\}}$ for small ϵ should not depend on the selected family of Hamiltonians $\{H_j\}$, as long as the second-order operator $\sum_{j=1}^f (\nabla_{H_j})^2$ is elliptic (in the above case on the torus, this is the Laplace operator $\frac{\partial^2}{\partial q^2} + \frac{\partial^2}{\partial p^2}$, which is indeed elliptic) [21].

3.3 Quantum coarse-grained propagator

We will now study the quantum analogue of P , that is the coarse-grained quantum propagator $\hat{P} = \hat{D} \hat{P}_M$. \hat{P} is still a Kraus superoperator, and therefore realizes a quantum Markov process: the quantum density evolves through the deterministic map $\text{ad}(\hat{M})$, then performs a random quantum jump through $\text{ad}(\hat{\Gamma}_{V \rightarrow \mathbb{N}})$, with a probability $1/K$ ($V \rightarrow \mathbb{N}$).

Linear combinations of quantum translations were already considered in [6] as models for decoherence on the quantum torus. The authors studied the evolution of densities through an operator similar with \hat{P} , by computing the time evolution of the ‘linear entropy’ $\text{tr}(\rho^2)$. They took for \hat{M} the quantized Baker’s map, which is a fully chaotic, yet discontinuous on \mathbb{T}^2 . More recently, similar computations were performed for smooth nonlinear perturbations of cat maps [16].

The superoperator \hat{P} is spectrally similar with its classical counterpart P . It conserves the trace: $\hat{P} \hat{\rho}_0 = \hat{\rho}_0$, but in contrast with its noiseless version \hat{P} , it has for unique invariant density $\hat{\rho}_0$, all other eigenvalues (in number $N^2 - 1$) being inside the unit disk. As a non-classical property, \hat{P} destroys purity: the image of a pure state $\hat{\rho} = |j\rangle\langle j|$ is not a pure state.

The following theorem, which is the central result of this paper, relates more precisely the spectra of \hat{P} and P in the semiclassical limit: it states the “semiclassical spectral stability” of coarse-grained propagators.

Theorem 1. *For any smooth map M on the torus and any fixed $\epsilon > 0$, the spectrum of the coarse-grained quantum propagator $\hat{P} = \hat{D} \hat{P}_M$ on L^2_N converges to that of the coarse-grained classical propagator $P = D P_M$ on $L^2(\mathbb{T}^2)$ in the semiclassical limit $N \rightarrow \infty$, uniformly in any annulus $R_r = \{r - \epsilon \leq |j| \leq r + \epsilon\}$ with $r > 0$.*

To compare the classical and quantum propagators, we use the isometry between the subspace I_N of $L^2(\mathbb{T}^2)$ and L^2_N , induced by Weyl quantization O_{P_N} and its inverse W^P (see section 3.1.1 for notations). \hat{P} is then isometric to $I_N(\hat{P}) \stackrel{\text{def}}{=} W^P \hat{P} O_{P_N}$ (I_N projects orthogonally $L^2(\mathbb{T}^2)$ onto I_N). We therefore need to compare the operators $I_N(\hat{P})$ and P on $L^2(\mathbb{T}^2)$. The crucial semiclassical estimate is the following lemma.

Lemma 1. *The finite-rank operators $I_N(\hat{P})$ converge to P in the operator norm on $L^2(\mathbb{T}^2)$, in the limit $N \rightarrow \infty$.*

Proof: The key semiclassical ingredient is Egorov’s property (13). From the norm inequality

$$\|k\|_{HS}^2 = \frac{1}{N} \text{tr}(\hat{V} \hat{V}) = \|k\|_{L^2(\mathbb{H}_N)}^2;$$

the convergence in (13) also holds for the Hilbert-Schmidt norm, that is on the space L^2_N . Inserting the symbol map W^P and noticing that for any $k \in Z^2$, $\|k\|_{I_N} \rightarrow \|k\|_{L^2}$ for large enough N , we now deal with operators on I_N , a subspace of $L^2(\mathbb{T}^2)$, so Egorov’s property may be recast in the form:

$$\|k\|_{L^2} \leq \|k\|_{I_N} + \epsilon \quad \forall k \in Z^2; \quad \|k\|_{I_N} = \|k\|_{L^2} + o(1) \quad \forall k \in Z^2.$$

Since M is a smooth map, the density P_M is smooth too, so that $I_N P_M \rightarrow P_M$ as $N \rightarrow \infty$. This means that the sequence of operators $I_N(\hat{P}_M)$ semiclassically converges to P_M in the *strong topology* on $B(L^2)$ (the bounded operators on $L^2(\mathbb{T}^2)$). Now, a standard lemma in functional analysis [9, Lemma 2.8] states that if a sequence A_n of bounded operators on some Banach space converge strongly to the operator A , then for any compact operator K , $K A_n$ converges to $K A$ in operator norm. Since D is compact, this implies that $D I_N(\hat{P}_M)$ converges to $D P_M$ in the operator norm. A simple comparison of the eigenvalues shows that $\|D I_N(\hat{P}) - D P_M\| \rightarrow 0$ as $N \rightarrow \infty$, which achieves to prove the lemma.

End of proof of the theorem: From lemma 1, one applies standard methods to show that the spectrum of $I_N(\hat{P})$ converges to that of P , as was done in section 2.1. Namely, for any nonzero (thus isolated) eigenvalue λ of P with spectral projector E_λ , and any $\epsilon > 0$ small enough, the spectral projector of the operator $I_N(\hat{P})$ in the disk $B(\lambda; \epsilon)$ satisfies $\|E_{B(\lambda; \epsilon)}^{(N)} - E_\lambda\| \rightarrow 0$ as $N \rightarrow \infty$. This means that both projectors have the

same rank for N large enough, and that the corresponding eigenstates are close to each other. The spectrum of \hat{P} is of course identical with that of P .

This spectral stability was noticed numerically in [26] for the kicked rotator on the 2-sphere. In their case, the coarse-graining consists in a sharp truncation of the Fourier expansion of the Husimi functions of the quantum densities, but the same arguments as above can be applied to show the spectral stability of the coarse-grained propagator in the semiclassical limit.

4 On the non-commutativity of the semiclassical vs. small-noise limits

In last section we have described the semiclassical limit of the quantum coarse-grained propagator \hat{P} for a *fixed* coarse-graining parameter $\epsilon > 0$, while section 2 was dealing with the small-noise limit $\epsilon \rightarrow 0$ for the classical propagator P .

These two limits do not commute. Indeed, for fixed $N \geq N_0$ the coarse-graining operator \hat{D} is a finite matrix, whose N^2 eigenvalues given in Eq. (18) satisfy $d_{\mathbf{k}}^{(N)} \neq 1$ as $\epsilon \rightarrow 0$. Therefore, in this limit $\mathbf{k} \hat{D} \mathbf{k} \neq 0$. For $\mathcal{K}(\mathbf{x})$ of compact support, we even have $\hat{D} = \text{Id}_{L_N^2}$ as soon as the rescaled support $(N)\text{Supp}(\mathcal{K})$ has no intersection with \mathbb{Z}^2 . This shows that for N fixed and ϵ decreasing to zero, \hat{P} is close to unitary on L_N^2 , uniformly with respect to the map M :

$$\forall \epsilon > 0 \exists N_0 \text{ s.t. } \forall N \geq N_0 \forall \mathbf{k} \in \mathbb{Z}^2 \quad |d_{\mathbf{k}}^{(N)} - 1| < \epsilon \quad (21)$$

On the opposite, there should exist a regime where $N \rightarrow \infty$ (semiclassical) and simultaneously $\epsilon = \epsilon(N) \rightarrow 0$ (vanishing noise) slowly enough, such that the eigenvalues of $\hat{P}^{(N)}$ stay close to the eigenvalues of $P^{(N)}$, and therefore behave differently according to the classical properties of M .

For an Anosov map, the “outer” eigenvalues (say, in some annulus R_r) will converge to the Ruelle resonances, while for an integrable map they form dense strings touching the unit circle. Eq. (21) shows that a *necessary* condition for \hat{P} to possess eigenvalues close to the origin (like P) is that the coarse-graining operator \hat{D} also has small eigenvalues. The smallest eigenvalues of \hat{D} correspond to the largest wave vectors in \mathbb{Z}_N^2 , namely $|\mathbf{k}| = N/2$. From the explicit expression (18), this implies the condition

$$N \epsilon(N) \gg 1 \quad (22)$$

This condition is quite obvious: it means that the scale of coarse-graining $\epsilon(N)$ must be larger than the “quantum scale” $\frac{1}{N} = \lambda \sim$, that is the “distance” between two nearby position states $\delta \mathbf{x} \sim \frac{1}{N}$. One may wonder if this condition is sufficient, or if $\epsilon(N)$ should decrease slower to get the desired spectral properties. We have so far no definite answer to this question for a general map.

In the next two subsections, we will compare the spectra of \hat{P} and P for the various maps treated classically in sections 2.1.1 and 2.2. We know no nonlinear Anosov map

for which Ruelle resonances can be computed analytically, so for this case we rely on the numerical studies [1, 26] of the perturbed cat map.

We plot some numerically-computed spectra, always using Gaussian noise and selecting two different \sim -dependences for the noise strength $\epsilon(N)$. We consider either a “slow decrease” $\epsilon(N) = N^{-1/2}$, for which the convergence to classical eigenvalues is checked even for the relatively small values of N (the largest value of N we considered is $N = 40$). To test the finer condition (25), we also consider a “fast decrease” of the noise $\epsilon(N) = \frac{\log(N)}{N}$, the convergence to stable eigenvalues being then harder to check.

We start by plotting on Fig. 1 (left) the spectrum of the quantum coarse-graining operator \hat{D} .

4.1 Quantum linear automorphisms

In this section, we will only consider maps A satisfying the “checkerboard conditions” given in section 3.1.2, necessary for their proper quantization on H_N . Then, the quantized linear automorphism \hat{A} satisfies the *exact* Egorov property [18]:

$$\hat{A}^k \hat{T}_{k=N} \hat{A}^{-1} = \hat{T}_{A^k k=N} \quad \hat{P}_A \circ \mathcal{P}_N(k) = \mathcal{P}_N(A^k k) = \mathcal{P}_N(A^k):$$

The quantum propagator therefore acts as a permutation on the quantum translations, like the classical propagator on plane waves (cf. Eq. (7)). The main difference between the quantum and classical frameworks comes from the fact that Weyl quantization \mathcal{P}_N is not one-to-one: $\mathcal{P}_N(k + Nk^0) / \mathcal{P}_N(k)$. As a result, each (infinite) orbit $\mathcal{O}(k) = \{A^t k; t \in \mathbb{Z}\}$ has to be taken modulo \mathbb{Z}_N^2 in the quantum case, yielding a finite “quantum orbit” $\mathcal{O}_N(k)$. Through a rescaling of $\frac{1}{N}$, $\mathcal{O}_N(k)$ is identified with a periodic orbit of A situated on the “quantum lattice” $(\frac{1}{N}\mathbb{Z})^2$. The period $T_{N,k}$ of this orbit is the smallest $t > 0$ such that $A^t k \equiv k \pmod{\mathbb{Z}_N^2}$. To compute the spectrum of P_A and $P_{\hat{A}}$ we need to analyze these quantum orbits.

The quantum orbits form a partition of \mathbb{Z}_N^2 , therefore a partition of the basis $\{f \hat{T}_{k=N}; k \in \mathbb{Z}_N^2\}$ of L_N^2 . To each $\mathcal{O}_N(k)$ corresponds the $T_{N,k}$ -dimensional subspace $\text{Span} \mathcal{O}_N(k)$, invariant through both \hat{P}_A and \hat{D} . The quantum propagator \hat{P}_A satisfies

$$\hat{P}_A^{T_{N,k}} \mathcal{P}_N(k) = \mathcal{P}_N(A^{T_{N,k}} k) = \mathcal{P}_N(k + Nv) = (1) \mathcal{P}_N(k) \quad (23)$$

for some $v \in \mathbb{Z}_N^2$, and $1 = k \wedge v + N v_1 v_2$. This implies that the eigenvalues of \hat{P}_A on $\text{Span} \mathcal{O}_N(k)$ are the phases $f \exp \frac{2i}{T} (r + 1/2)$; $r = 0; \dots; T-1$ (we abbreviate $T_{N,k}$ with T). By switching on the noise, the equation (23) is modified by inserting the action of \hat{D} on the successive modes $\hat{T}_{A^t k=N}$. As a result,

$$\hat{P}_A^T \hat{T}_{k=N} = (1) d_{\mathcal{P}_N(k)}^{(N)} \hat{T}_{k=N};$$

with

$$d_{\mathcal{P}_N(k)}^{(N)} \stackrel{\text{def}}{=} \sum_{t=0}^{T-1} d_{\hat{A}^t k}^{(N)};$$

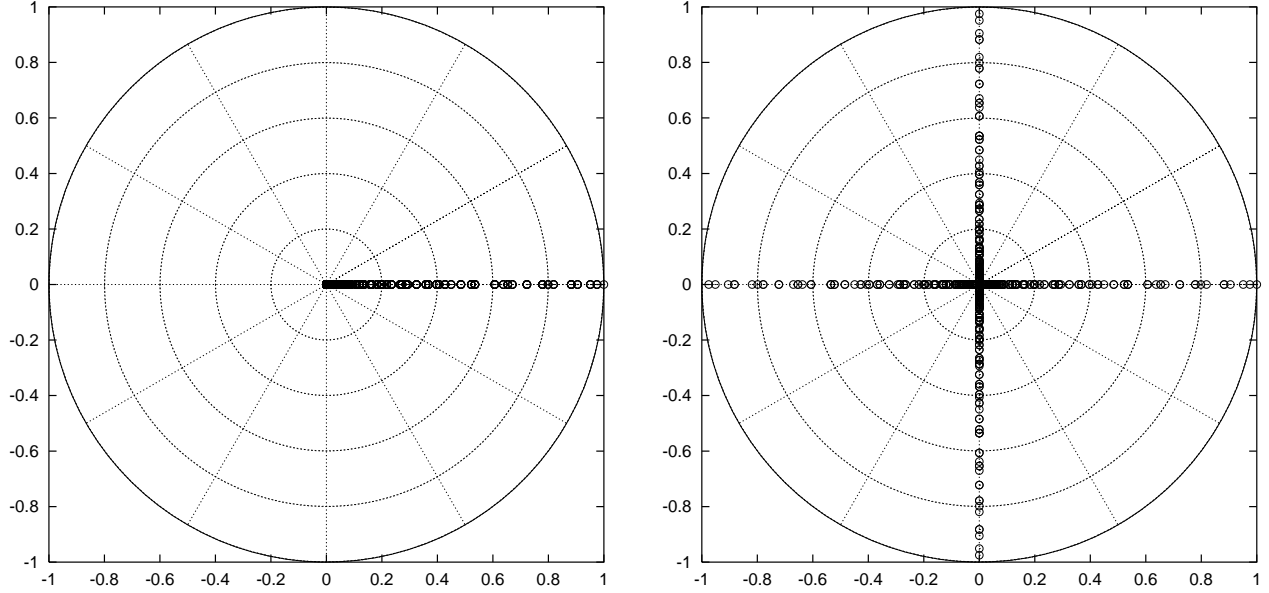


Figure 1: Spectrum of the quantum coarse-graining operator \hat{D} for the Gaussian noise (left); Spectrum of the coarse-grained $=2$ -rotation $\hat{P}_{\mathcal{J}}$ (right). Parameters are $N = 40$, $\epsilon = N^{-1/2}$ (small circles). The large concentric circles are only shown for clarity.

The spectrum of \hat{P} on $\text{Span} \mathcal{O}_N(\mathbf{k})$ thus consists in T regularly spaced points on the circle of radius $\mathfrak{d}_{\rho(\mathbf{k})}^{(N)j} \stackrel{\text{def}}{=} \mathfrak{d}_{\rho(\mathbf{k})}^{j=T}$. To estimate this radius

$$\frac{1}{T} \log \mathfrak{d}_{\rho(\mathbf{k})}^{(N)j} = \frac{1}{T} \sum_{\mathbf{k} \in \mathcal{O}_N(\mathbf{k})} \log \mathfrak{d}_{\mathbf{k}^0}^{(N)j} \quad (24)$$

According to Eq. (18), this quantity is the average over the periodic orbit $\frac{1}{N} \mathcal{O}_N(\mathbf{k})$ of the function $f_{\mathbf{k}}(N; j) \stackrel{\text{def}}{=} \log \frac{\kappa(N; j)}{\kappa(N; 0)}$. This function is smooth in j except at possible logarithmic singularities if κ vanishes. In the Gaussian case $G(\mathbf{x}) = e^{-\mathbf{x}^2}$, f_G has no singularities and admits for $N \gg 1$ the asymptotic behaviour $f_G(N; j) \sim \frac{1}{2} \log \frac{N^2}{j^2}$ in the square $\frac{1}{2} \leq j \leq \frac{1}{2} N$.

We have obtained an explicit relationship between the spectrum of $\hat{P}_{\mathcal{A}}$ and the structure of periodic orbits of A on the quantum lattice. The latter structure drastically differs between chaotic and integrable automorphisms, which leads to qualitatively different quantum spectra. Below, we sketch the description of these quantum orbits, respectively for the elliptic, parabolic and hyperbolic maps. We use the notations and results of sections 2.1.1, 2.2.2.

4.1.1 Elliptic transformation \mathcal{J}

The quantization of the $=2$ -rotation \mathcal{J} yields the finite Fourier transform $\hat{\mathcal{J}}$. The classical orbits $\mathcal{O}(\mathbf{k})$ are of period 4. In general, the successive $\mathcal{J}^j \mathbf{k}$ are not congruent mod N , so

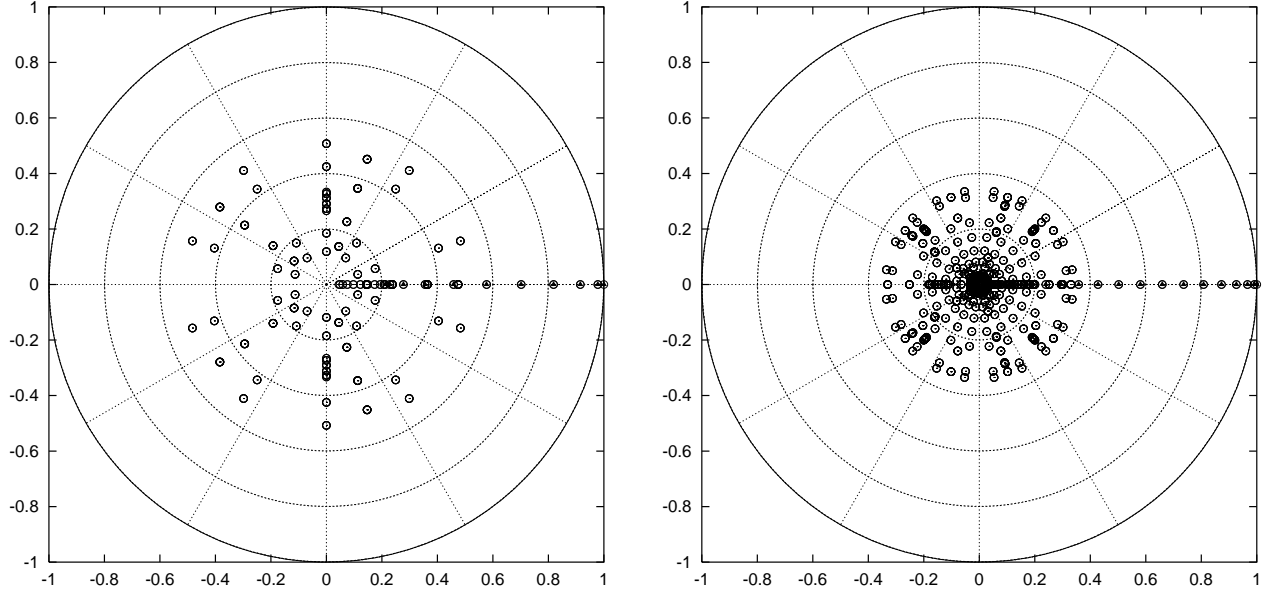


Figure 2: Spectrum of \hat{P}_{S_2} for the linear shear S_2 (circles) and values $\text{fd}_{(j,0)}^{(N)} \mathfrak{g}_{j=0}^N$ (triangles). Parameters are $N = 20$ (left), $N = 40$ (right) and in both cases $\mathfrak{g} = \log(N) = N$.

that the quantum orbit $O_N(\mathbf{k})$ also has period 4. The only exception occurs for N even, $\mathbf{k} = (\frac{N}{2}; \frac{N}{2})$ (period 1) or $\mathbf{k} = (0; \frac{N}{2})$ (period 2). Assuming that the coarse-graining kernel has the symmetry $\mathcal{K}(\cdot) = \mathcal{K}(\mathcal{J}\cdot)$, the eigenvalues of \hat{P}_{S_2} on a 4-dimensional $\text{Span}O_N(\mathbf{k})$ are $\text{fd}_{\mathbf{k}}^{(N)}; l=0; \dots; 3\mathfrak{g}$. Taking all quantum orbits into account, the spectrum forms 4 strings as in the classical case (see Fig. 1, right). For a Gaussian noise, Eq. (19) shows that these eigenvalues are exponentially close to the corresponding classical eigenvalues.

4.1.2 Parabolic linear shear S

We can quantize properly the parabolic shear S described in section 2.2.2 if the integer s is even. The space of P_S -invariants $V_{\text{inv}} = \text{Span}\{f_{(l,0)}; l \in \mathbb{Z}\} \subset \mathfrak{g}$ quantizes to the \hat{P}_S -invariants $V_{\text{inv};N} = \text{Span}\{\hat{T}_{(\frac{l}{N},0)}; l \in \mathbb{Z}_N\} \subset \mathfrak{g}$. Each $\hat{T}_{(\frac{l}{N},0)}$ is eigenstate of \hat{P} with eigenvalue $d_{(0;l)}^{(N)}$, which is close to the classical eigenvalue $\mathcal{K}((0;1))$ in the semiclassical limit. If $N \gg 1$, these eigenvalues form a string connecting unity to the origin.

Now we study the spectrum of \hat{P} on the orthogonal of the invariant space, $V_{\text{inv};N}^\perp$. For $\mathbf{k} = (k_1; k_2)$ with $k_2 \not\equiv 0 \pmod{N}$, the infinite orbit $O(\mathbf{k}) = \{k + (jsk_2; 0); j \in \mathbb{Z}\} \subset \mathfrak{g}$ projects modulo N onto a finite orbit $O_N(\mathbf{k})$ whose period depends on the “step” $\mathfrak{g} \stackrel{\text{def}}{=} \gcd(N; sk_2)$: $O_N(\mathbf{k}) = \{k + (j\mathfrak{g} \pmod{N}; k_2); j = 0; \dots; \frac{N}{\mathfrak{g}} - 1\}$. For a fixed $k_2 \in \mathbb{Z}$, the step \mathfrak{g} stays bounded in the limit of large N , so that the sum (24) behaves as the integral $\int_0^1 dt f_{\mathbf{k}}(N; (t; \frac{k_2}{N}))$. For the Gaussian noise, the latter yields $\frac{1}{2}(\frac{N^2}{12} + k_2^2) + o(1)$. For a general value of $k_2 \in \mathbb{Z}_N \setminus \{0\}$, \mathfrak{g} may be of order N (or even equal to N , leading to a quantum invariant mode outside $V_{\text{inv};N}$), in which case the sum (24) is not well-approximated by an

integral, but one can (for Gaussian noise) prove the uniform upper bound:

$$8k \leq \sum_{N=1}^{\infty} \frac{1}{T_N} \log \sum_{j=0}^{(N)} \rho_{(k)}^j \leq C (N^2)$$

with $C = \inf_{1 \leq s \leq 16} \frac{1}{s}$. The eigenvalues of \hat{P} on V_{inv}^2 are therefore situated on circles of radii $e^{-C(N)^2}$, so they uniformly converge to the origin as $N \rightarrow \infty$ (the origin was the spectrum of the P_{ρ} acting on V_{inv}^2).

In Fig 2 we show the spectra of \hat{P}_{S_2} for the shear $S_2 = \begin{pmatrix} 1 & 2 \\ 0 & 1 \end{pmatrix}$ and a “fast decreasing noise”, together with the values $\sum_{j=0}^{(N)} \rho_{(j;0)}^j$. The ‘non-invariant spectrum’ converges slowly to the origin, while the ‘invariant spectrum’ becomes dense on the interval $[0;1]$. Had we chosen a larger noise, the non-invariant spectrum would be contained in a smaller disk for the same values of N .

4.1.3 Hyperbolic transformations

The periodic orbits of a hyperbolic automorphism A were thoroughly studied in [31]; the authors classified the orbits according to the \mathbb{Z}^2 sublattice they belong to. Yet, they gave no equidistribution estimate on long periodic orbits.

Our aim is to estimate the RHS of Eq. (24) for all quantum orbits, at least for large enough N (we will restrict ourselves to the Gaussian coarse-graining). For any Anosov map, the long periodic orbits equidistribute in the statistical sense (averaging over all orbits of a given period) in the limit of long periods [30]. For a certain class of hyperbolic automorphisms, semiclassical equidistribution of *all* quantum orbits was obtained for an infinite subsequence of values of N [15]. Equidistribution morally implies that the sum (24) behaves as the integral $\int_{\mathbb{T}^2} dx f_G(N; x) \sim \frac{(N)^2}{6}$. One can indeed show that for N in this subsequence, the eigenvalues of \hat{P}_A on \wedge_0^2 have moduli $\exp \left(-\frac{(N)^2}{6} + O(N^{-3}) \right)$.

There also exist arbitrary large values of N for which the period $T(N)$ of A modulo N is as small as $\frac{2 \log N}{\lambda} + O(1)$, where $\lambda > 0$ is the Lyapunov exponent of A [31]. All quantum orbits $O_N(k)$ have periods dividing $T(N)$. Starting from $k_0 = (0;1)$, the linear dynamics shows that the point $\frac{A^{t k_0}}{N}$ remains close to the origin (that is, at a distance $\ll 1$) along the unstable direction until the time $\frac{\log N}{\lambda}$, when it reaches the boundary of the square $[j_1; j_1 + 2; j_2; j_2 + 2]$; it is then straight away ‘captured’ by the stable manifold, which brings it back to the origin during the remaining $\frac{\log N}{\lambda}$ steps. This orbit thus achieves an “optimally short” homoclinic excursion from the unstable origin, and is far from being equidistributed. The average of f_G along this orbit is of order $\frac{C(N)^2}{\log N}$, so the eigenvalues of \hat{P}_A on $\text{Span} O_N(k_0)$ have a radius $\exp \left(\frac{C(N)^2}{\log N} \right)$. These eigenvalues will therefore converge to the origin under the condition

$$\frac{N}{\log N} \rightarrow \infty \quad (25)$$

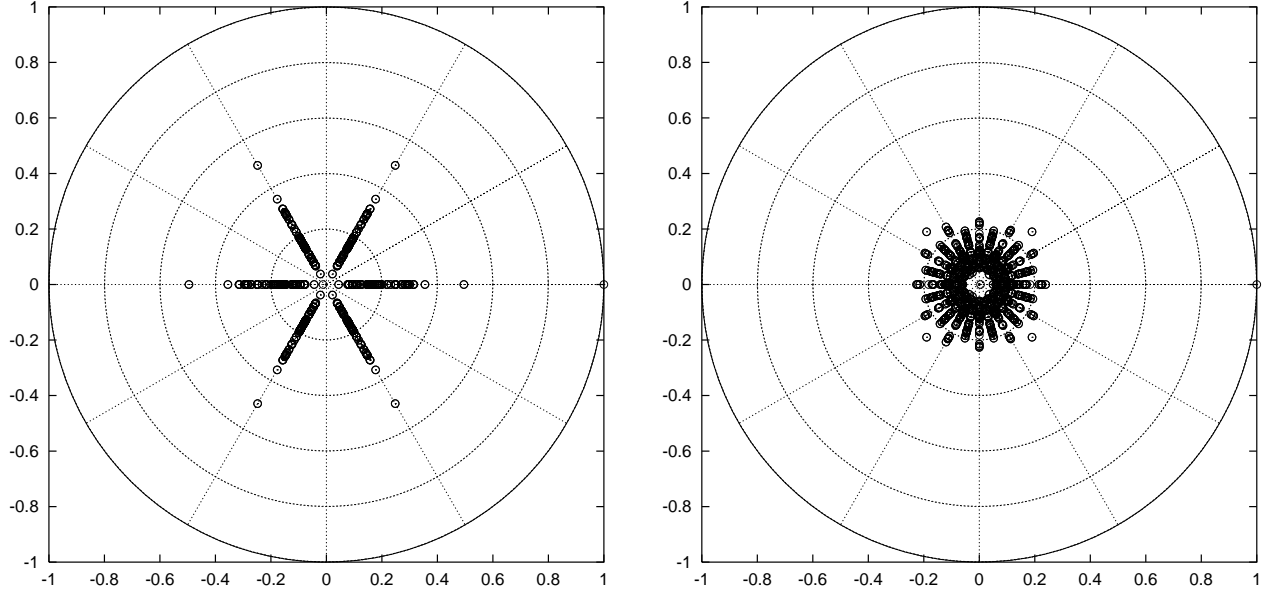


Figure 3: Spectrum of $\hat{P}_{\mathcal{A}_0}$ for the cat map \mathcal{A}_0 . Parameters are $N = 30$ (left), $N = 40$ (right) and in both cases $\ell = \log(N) \approx N$. $N = 30$ corresponds to a “short quantum period” $T(30) = 6$, which is clearly visible on the shape of the spectrum.

We believe that these particular values of N represent the “worst case” as far as equidistribution of long orbits is concerned, and that condition (25) suffices for the spectra of $\hat{P}_{\mathcal{A}}$ to semiclassically converge to the origin for the full sequence $N \rightarrow \infty$. In Fig. 3 we show the spectrum of $\hat{P}_{\mathcal{A}_0}$ for the quantization of the cat map $\mathcal{A}_0 = \begin{pmatrix} 2 & 1 \\ 3 & 2 \end{pmatrix}$, with the fast decreasing disorder.

Remark: For both the parabolic shear and the hyperbolic automorphisms, the spectrum of \hat{P} on $V_{\text{in}}^{\mathbb{Z}^2}$ reduces to $\ell_0 \mathfrak{g}$ if the coarse-graining consists in a sharp truncation in Fourier space, and ℓ_1 grows as $\ell_1 \propto N$ with c a finite but small constant (depending on the classical map). Any nontrivial quantum orbit $\mathcal{O}_N(\mathbf{k}_0)$ then contains an element \mathbf{k} s.t. $|\mathbf{k}| > \ell_1$, such that the corresponding mode $\hat{T}_{\mathbf{k}=\mathbf{N}}$ is killed by \hat{D} .

4.1.4 Quantum translations

As we mentioned in section 3.1.2, any classical translation $T_{\mathbf{v}}$ with $\mathbf{v} \in \mathbb{T}^2$ can be quantized on any H_N by the quantum translation $\hat{T}_{\mathbf{v}^{(N)}}$, where $\mathbf{v}^{(N)}$ is the “closest” point to \mathbf{v} on the quantum lattice. This quantization was shown [27] to satisfy Egorov’s property (13).

From Eq. (17), the quantum propagator $\hat{P}_{\mathbf{v}^{(N)}} = \text{ad}(\hat{T}_{\mathbf{v}^{(N)}})$ admits any quantum translation $\hat{T}_{\mathbf{k}=\mathbf{N}} = \mathcal{O}_{\mathbb{P}^N}(\mathbf{k})$ as an eigenstate, with eigenvalue $e^{2i \mathbf{v}^{(N)} \wedge \mathbf{k}}$. All eigenvalues are N -th roots of unity, and are least N -degenerate; in case the classical translation $T_{\mathbf{v}}$ is ergodic, these degeneracies contrast with the nondegenerate (but dense) spectrum of $P_{\mathbf{v}}$.

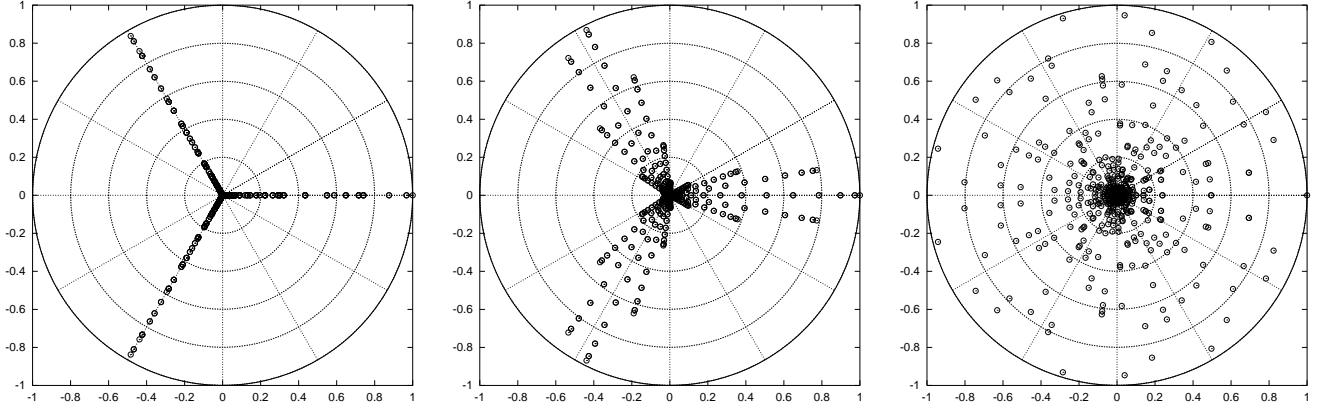


Figure 4: Spectrum of \hat{P}_v for the translations $v = (0; \frac{1}{3})$ (left: $N = 30$, center: $N = 37$) and $v = (\frac{1}{2}; \frac{1}{5})$ (right: $N = 37$). The noise strength is $\epsilon = N^{-1/2}$. For the rational translation, the eigenvalues are either exactly on the classical axes (for N multiple of 3), or semiclassically converge to it. For the irrational one, the eigenvalues become dense in the full disk.

On the opposite, for a rational translation (the classical eigenvalues form a finite set), the quantum eigenvalues may take values in all N -th roots of unity, in case N and $v^{(N)}$ are coprime. The spectra of P_v and $\hat{P}_{v^{(N)}}$ may thus be qualitatively very different.

This difference disappears when one switches on the noise. Each quantum translation is also an eigenstate of the coarse-grained propagator $\hat{P}_v = \hat{D} \hat{P}_{v^{(N)}}$, associated to the eigenvalue $e^{2i k \wedge v^{(N)}} d_{jk}^{(N)}$. In the semiclassical limit, the deviation from the corresponding classical eigenvalue $e^{2i k \wedge v} K(k)$ (cf. section 2.2.1) depends on both the wavevector k and the difference $v - v^{(N)}$.

To give an example, the rational translation vector $v = (0; \frac{1}{3})$ leads to 3 eigenvalues $e^{2i k \wedge v}$ for the classical propagator P_v , and 3 (infinite) strings for the spectrum of P_v . Quantum-mechanically, if N is a multiple of 3 one takes $v^{(N)} = v$, and the eigenvalues of \hat{P}_v are exponentially close to the classical ones (Fig. 4, left). In the case $N = 3n + 1$, the quantum translation vector will be $v^{(N)} = (0; \frac{n}{3n+1})$, so that the classical and quantum noiseless eigenvalues for the mode k deviate of an angle $2 k \wedge (v - v^{(N)}) = \frac{2 k_1}{3N}$: this can be as large as ≈ 3 for wavevectors $|k_1| \approx N/2$. After switching on the noise, the classical and quantum eigenvalues for $k \in \mathbb{Z}_N^2$ can deviate by at most $O(\frac{1}{N})$, the maximal deviations occurring for wavevectors $|k_1| \approx 1, k_2 = O(1)$ (Fig. 4, center).

4.2 Examples of quantized nonlinear maps

In this section we shortly review the spectrum of quantized coarse-grained propagators for three nonlinear maps: we first treat the nonlinear parabolic shear of section 2.2.3 and the stroboscopic map of the Harper Hamiltonian (section 2.2.4), for which we have some analytic handle. We then consider a perturbed cat map and compare the numerically computed eigenvalues of \hat{P} to the ones of P obtained in [1].

the nonlinear shear described in section 2.2.3 is quantized by taking the product of the quantum linear shear \hat{S} (see section 4.1.2) with the matrix $e^{i\hat{F}=\sim}$. Since $F(\mathfrak{p})$ is a function of the impulsion only, its Weyl quantization \hat{F} acts diagonally on the impulsion basis $\mathfrak{f}\mathfrak{p}_j\mathfrak{g}$. As a result, the perturbation $\text{ad}(e^{i\hat{F}=\sim})$ acts trivially on any projector $\mathfrak{p}_j\mathfrak{i}\mathfrak{p}_j$ and therefore on any invariant translation $\hat{T}_{(0,\mathfrak{m})=\mathfrak{N}}$. As a result, the spectrum of the noisy nonlinear propagator on $V_{\text{in}V,\mathfrak{N}}$ forms the same string as for the linear shear.

The action of \hat{P} on $V_{\text{in}V,\mathfrak{N}}$ can be studied as in the classical case: due to the nonlinear perturbation, the propagator is not merely a permutation, but acts inside each subspace $V_{n,\mathfrak{N}} = \text{Span}\mathfrak{f}\hat{T}_{(n,\mathfrak{m})=\mathfrak{N}}; \mathfrak{m} \in \mathbb{Z}_N \mathfrak{g}$ as a unitary $N \times N$ Toeplitz matrix $\hat{P}^{(n)}$. In Appendix A.2 we study the non-unitary spectrum of $\hat{P}^{(n)}$ when taking for $\mathcal{K}(\cdot)$ a sharp cutoff function: $\hat{P}^{(n)}$ is therefore the truncated matrix to the subspace $\mathfrak{f}\mathfrak{m} \in \mathbb{Z}_N \mathfrak{g}$. We compare this truncated propagator with the corresponding classical one, and show that if $\mathfrak{N} \gg 1$, both spectra converge to the same union of 1-dimensional strings contained in a fixed ‘small’ disk around the origin, the size of which depends on the strength of the perturbation F^0 . The spectrum of \hat{P} for the quantized nonlinear shear $e^{i\hat{F}=\sim} \hat{S}_2$ with $\hat{F} = \frac{0.25}{2} \cos(2\mathfrak{p})$ is shown in Fig. 5 (left) for $N = 40$ and $\mathfrak{N} = \log(N) = 5$, together with the values $\mathfrak{f}\mathfrak{d}_{(j;0)}^{(N)} \mathfrak{g}_{j=0}^{\mathfrak{N}}$.

The quantization of the stroboscopic map \hat{A}_H for the Harper flow, *i.e.* the unitary matrix $e^{i\hat{H}=\sim}$, leads to the propagator \hat{P}_H leaving invariant any density of the type \hat{H}^n . Similarly to what happens for the classical propagator (cf. section 2.2.4), under the same conditions for coarse-graining kernel $\mathcal{K}(\cdot)$, \hat{P}_H admits for eigenstates \hat{H} , $(\hat{H}^2 - \text{Id})$ and $\hat{H}^3 - \frac{7+2\cos(2\mathfrak{N})}{4} \hat{H}$, and the associated eigenvalues $\mathfrak{f}\mathfrak{d}_{(j;0)}^{(N)} \mathfrak{g}_{j=1}^3$ converge to the classical eigenvalues $\mathfrak{f}\mathcal{K}(j) \mathfrak{g}_{j=1}^3$ if $N \gg 1$. The spectrum of \hat{P}_H for $N = 40$ and $\mathfrak{N} = N^{1/2}$ is shown in Fig. 5 (right), together with the values $\mathfrak{f}\mathfrak{d}_{(j;0)}^{(N)} \mathfrak{g}_{j=0}^4$. For the Gaussian noise we are using, only \hat{H} is an eigenstate of \hat{D} , so the following eigenvalues are hybridized by the coarse-graining. A ‘string’ of eigenvalues along the positive real axis is clearly visible on the plot.

We consider the quantization of the perturbed cat map studied in [1], that is the map $A_{n1} : \mathfrak{q} \mapsto \mathfrak{p} \begin{pmatrix} 2\mathfrak{q} + \mathfrak{p} \\ 3\mathfrak{q} + 2\mathfrak{p} + \cos(2\mathfrak{q}) \cos(4\mathfrak{q}) \end{pmatrix}$. We selected the perturbation $\mathfrak{N} = 0.5 = 2$ in order to compare the quantum spectrum with the classical resonance spectrum described in [1, Fig. 2]. In Figure 6 we plot the spectrum of \hat{P} for $N = 40$ together with the 7 ‘outer’ resonances whose values are given in [1, Table I]; in the ‘large noise’ regime (left), the largest quantum eigenvalues are indeed close to these resonances, and the rest of the spectrum inside a smaller disk. The small-noise regime (right) does not uncover the classical resonances, however the non-invariant spectrum is already contained in a relatively small disk around the origin, of radius comparable with the largest resonance.

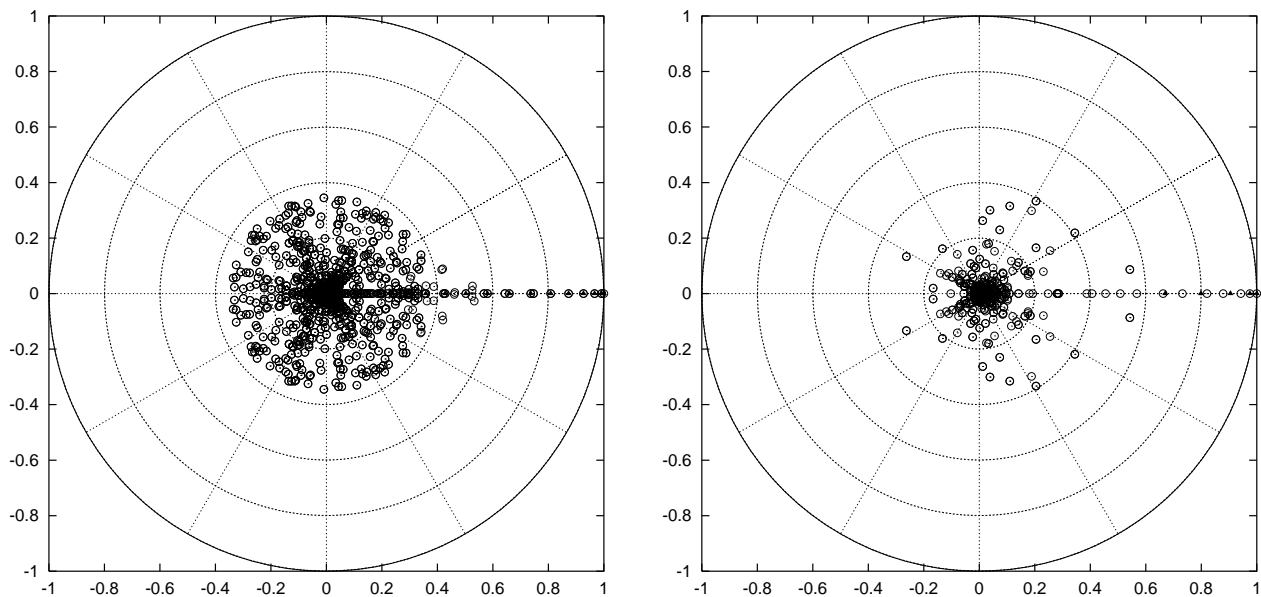


Figure 5: Spectrum of \hat{P} for the nonlinear shear $e^{i\hbar\hat{S}_2}$ (left, $N = 40$, $\hbar = \log(N)/N$) and the Harper map $e^{i\hbar\hat{H}}$ (right, $N = 40$, $\hbar = N^{-1/2}$). In both cases we also plotted some values $d_{j;0}^{(N)}$ (black triangles).

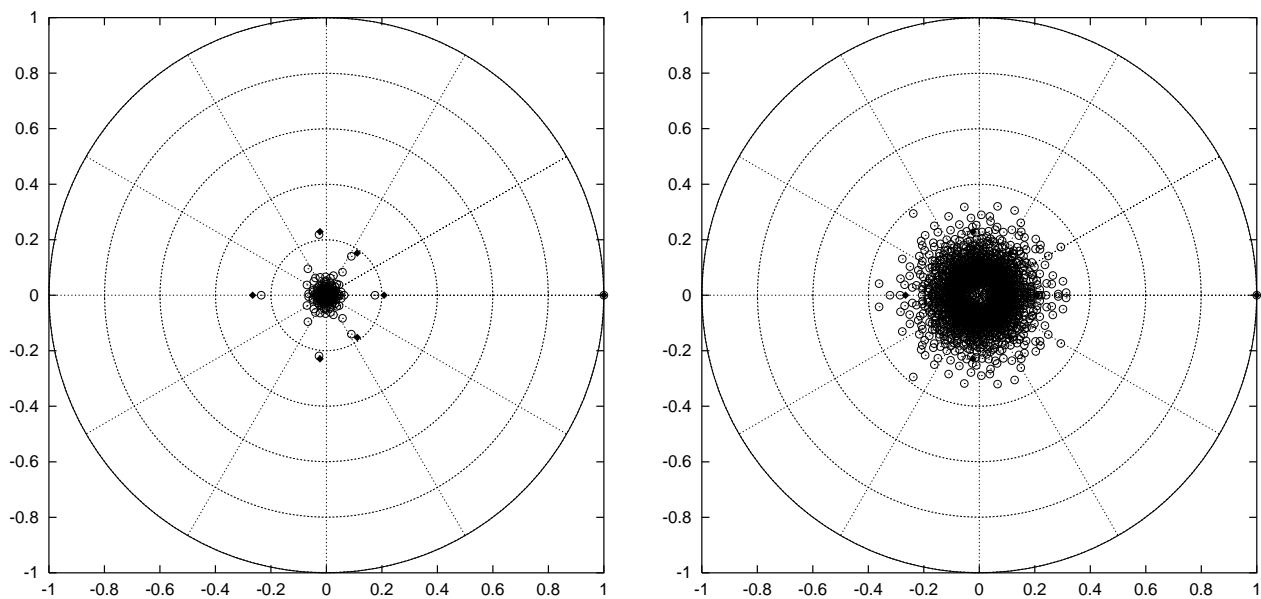


Figure 6: Spectrum of \hat{P} for the quantum perturbed cat map \hat{A}_{n1} (empty circles) together with the largest 7 classical resonances (black diamonds). Left: $N = 40$, $\hbar = N^{-1/2}$. Right: $N = 40$, $\hbar = \log(N)/N$.

Concluding remarks

In spite of the relatively low values of N used in the numerical plots, one can already clearly distinguish the two different behaviours of the quantum spectra, depending on the classical motion, especially for the slow noise decrease $\epsilon = N^{-1/2}$. For the integrable maps, the largest nontrivial eigenvalue of the noisy quantum propagator \hat{P} is at a distance ϵ^2 from unity, and this eigenvalue is the first one of a string of eigenvalues connecting unity with a neighbourhood of the origin. On the opposite, for the two chaotic maps we studied (linear and perturbed cat maps), the spectrum already shows a finite gap for these values of N , even in the fast-decreasing noise regime $\epsilon = \log(N)/N$; however, for the value of N used, the gap is governed by the classical resonances only in the regime of larger noise $\epsilon = N^{-1/2}$. I conjecture that the quantum spectrum also converges to the classical spectrum (in any annulus R_r) in the regime $\epsilon = \log(N)/N$, this being visible only for much higher values of N .

General conclusion

In this paper we have shown the connection between the spectra of coarse-grained quantum and classical propagators for maps on the 2-dimensional torus. I claim that theorem 1 can be straightforwardly extended to maps on any compact phase space, like the 2-sphere S^2 used in [26, 22]. Using our knowledge of the spectrum of the classical noisy map, one infers the presence or the absence of a *finite gap* between the (trivial) eigenvalue unity on the one hand, the rest of the spectrum on the other hand, taking both the semiclassical ($\hbar \rightarrow 0$) and small noise ($\epsilon \rightarrow 0$) limits in a well-defined way. The presence of this gap in the classical noisy propagator is related with the ergodic properties of the map. On one extreme, corresponding to integrable maps with an infinitely dimensional invariant subspace, there is no gap in the small-noise limit, and the spectrum contains a dense ‘string’ of eigenvalues connecting unity with the interior of the disk: the long-time evolution is therefore governed by the eigenmodes associated with these large eigenvalues, and is typically of *diffusive type*. On the opposite extreme, for M an Anosov map (“strongly chaotic”), the spectrum exhibits a finite gap, responsible for the (classical) exponential mixing. The case of maps with less chaotic behaviour is far from being settled. The example of irrational translations shows that ergodicity does not imply the presence of a gap. Exponential mixing was recently proven for some non-uniformly or partially hyperbolic maps (see [4] for a review of recent results), but it is not clear (to me) whether it automatically implies a gap in the spectrum of \hat{P} , although it is quite plausible. Maps with *subexponential* mixing would also deserve to be studied from this point of view.

Like in the classical framework, the presence of a gap in the spectrum of the quantum noisy propagator allows to describe the long-time dynamics of densities induced by this operator $\hat{\rho}(t) = \hat{P}^t \hat{\rho}(0)$. This dynamics is a possible model for a dissipative perturbation of the unitary evolution $\hat{U} = \hat{M}^t \hat{M}^\dagger$, the dissipation being induced by the interaction with the environment [6]. One measure of the decoherence occurring through this evolution

is the “purity”, or “linear entropy” $H(\rho) = -\text{tr}(\rho \ln \rho)$. For an Anosov map M , the evolution of this entropy for large times will be governed by the largest nontrivial eigenvalues of \hat{P} , which are semiclassically close to the classical resonances. This very evolution was recently studied for perturbed quantum cat maps, allowing to estimate the first resonances of \hat{P} for large values of N [16].

The noise operator used in all the paper consisted in an average over random translations in phase space. To diagonalize this operator, we have used the fact that the classical (resp. quantum) propagators for translations P_v (resp. \hat{P}_v) form a commutative algebra, and admit as eigenfunctions the Fourier modes. We obtained explicit expressions for the spectrum of P_M for the class of linear maps M , because these maps acted simply on these Fourier modes. However, as noticed in section 3.2.3, one may be interested in a more general type of diffusion operator, like the one defined in Eq. (20). The spectrum of D^{FH}_{jg} for a given map M should be qualitatively independent on the family of Hamiltonians FH_{jg} , as long as the operator D^{FH}_{jg} has the same characteristics as the coarse-graining D , namely it leaves almost invariant some “soft modes”, whereas fast-oscillating modes are rapidly damped. In particular, for M an Anosov map, the outer spectrum of D^{FH}_{jg} should converge to the set of resonances f_{jg} , and the rest be contained in a smaller disk, in the limit $\epsilon \rightarrow 0$. For an integrable map, the eigenvalues will not pointwise converge to the ones of \hat{D} , but they should also accumulate along a ‘string’ touching unity.

Our choice for the superoperator \hat{D} was inspired by its classical analogue, as well as its relevance to modelize the “quantum noise”. However, in some quantum mechanical systems experiencing (weak) interaction with the environment, the effective “noise” or “decoherence” superoperator may have no obvious classical analogue; this seems to be the case for instance in Nuclear Magnetic Resonance experiments performed in order to construct a “quantum computer”[29]. The quantum Hilbert space is composed of a sequence of M spins, so it is isomorphic with the torus Hilbert space H_N for $N = 2^M$ (each spin corresponds to a *binary digit* of the position α_j). The decoherence operator acting on such a system (for a small number of spins) has been experimentally measured, it seems to be the product of operators acting independently on the individual spins, and therefore does not enter in the family of diffusion operators described above; in particular, such a decoherence operator seems to have no obvious classical counterpart. Conjugating this type of decoherence operator with a unitary evolution (typically, the finite Fourier transform \hat{J}) may lead to a drastically different spectrum from the one shown in Fig. 1 (right), not excluding the presence of a gap.

Acknowledgements: I thank M. Zirnbauer and the Institut für theoretische Physik, Universität zu Köln, where this work was initiated. I am grateful to V. Baladi for pointing out ref. [7] to me, and thank S. Keppeler for his insight on integrable maps. I had interesting discussions on the whole subject with M. Saraceno and I. Garcia Mata.

A Appendix

A.1 Classical nonlinear shear: spectrum of truncated Toeplitz matrices

This appendix describes the spectrum of the noisy classical propagator for a nonlinear shear (section 2.2.3). In each invariant subspace $V_n = \{e^{2i n q}(\rho)g(n \in \mathbb{Z})\}$, the Perron-Frobenius operator P acts as a multiplication of the function $a_n(\rho)$ on the circle $T \ni t = e^{2i p}$ by:

$$a_n(e^{2i p}) \stackrel{\text{def}}{=} e^{2i n (sp + F^0(\rho))} = \prod_{m \in \mathbb{Z}} a_n(m) e^{2i m p} : \quad (26)$$

Notice that $a_n(t) = (a_1(t))^n$. In the Fourier basis, this multiplication has the form of an infinite Laurent matrix $L(a_n)$, with entries $L(a_n)_{ij} = a_n(i - j)$. From standard results, the spectrum of $P|_{V_n}$ is absolutely continuous, with support the range of the function $a_n(t)$ (here, the unit circle).

We consider the coarse-graining consisting in a sharp truncation in Fourier space: $\mathcal{K}(\cdot) = (\cdot)_1 (\cdot)_2$. The noisy propagator P then acts on V_n as the matrix $L(a_n)$ truncated to the block $\{j_n \leq j \leq j_n + 1\}g$, or equivalently as $\{1 \leq m \leq m^0 + 1\}g$. We assume that the smooth function $a_n(t)$ on T can be continued to an analytic (or meromorphic) function on \mathbb{C} (for the linear shear, one has $a_n(z) = z^{-sn}$). Then [9, Prop. 2.17 and Section 5.8], for any $r > 0$ and any $\epsilon > 0$, the spectrum of this truncated matrix is contained in the *convex hull* of the curve $a_n(rT)$. For the linear shear, these curves are the circles centered at the origin, so the spectrum reduces to $\{0\}g$, as expected. If the perturbation F^0 is small, these curves are deformations of circles, some of which remain in a small neighbourhood of the origin. As a concrete example, the perturbation $F(\rho) = \frac{1}{2} \cos(2\rho)$ leads to the function $a_1(z) = z^s \exp\{f(1=z+z)\}g$. The curves $a_1(rT)$ satisfy

$$8r > 0; \{j \leq j = r\} \{a_1(z) \leq r^s \exp(\{j \leq r - r\})\}:$$

We assume that $s > 0$. For a small perturbation ($\epsilon \ll 1$), the function on the RHS has a minimum of value $a_{\text{min}}(\cdot) = \frac{\epsilon}{s} e^{-s}$. This implies that for any n , the spectrum of $P|_{V_n}$ is contained in the disk of radius $a_{\text{min}}(\cdot)^{j_n}$ for any $\epsilon > 0$ (we have used the symmetry $a_n = \overline{a_n}$).

For a more general perturbation $2 F^0(t) = \prod_{m=1}^M f_m t^m + c \cdot c$: one can use the bound $2 \{F^0(rt)\} \leq \sup(g(r); g(1=r))$, with $g(r) \stackrel{\text{def}}{=} \prod_{m=1}^M f_m r^m$. If $g(r)$ is “small”, then the function $r^s \exp(g(1=r))$ has a minimum value $a_{\text{min}} \ll 1$ on \mathbb{R}_+ . This implies that the spectrum of $P|_{V_n}$ is contained, for any ϵ , in the disk around the origin of radius $a_{\text{min}}^{j_n}$.

A.2 Quantum nonlinear shear

The results of the previous appendix can be easily adapted to the quantized nonlinear shear. The latter is defined as the composition of the quantum linear shear \hat{S} with the Floquet operator corresponding to the Hamiltonian \hat{F} (see Section 2.2.3): the quantum

map therefore reads $\hat{S} e^{2iN\hat{F}}$. Its action is diagonal in the impulsion basis $\{ \mathbf{p}_j \}_{j \in \mathbb{Z}_N}$ of H_N ($\mathbf{p}_j = \frac{j}{N}$, with $j \in \mathbb{Z}_N$):

$$\hat{S} e^{i\hat{F} = \sim} \mathbf{p}_j \mathbf{i}_N = e^{2iN \left(\frac{s}{2} p_j^2 + F(p_j) \right)} \mathbf{p}_j \mathbf{i}_N :$$

Since s is even, this expression is well-defined for any $j \in \mathbb{Z}_N$. It allows to express the action of the corresponding propagator \hat{P} on the quantum translations $\hat{T}_{k=N}$, with $k = (m; n) \in \mathbb{Z}_N^2$. Such a translation can be decomposed as

$$\hat{T}_{k=N} = \sum_{j \in \mathbb{Z}_N} \mathbf{p}_{j+n} \mathbf{i} \mathbf{p}_j \mathbf{j} e^{2i m \left(p_j + \frac{n}{2N} \right)} :$$

\hat{P} acts inside each subspace $V_{n,N} = \text{Span} \{ \hat{T}_{(m;n)=N} ; m \in \mathbb{Z}_N \} = \text{Span} \{ \mathbf{p}_{j+n} \mathbf{i} \mathbf{p}_j \mathbf{j} ; j \in \mathbb{Z}_N \}$. The propagator \hat{P} indeed multiplies each $\mathbf{p}_{j+n} \mathbf{i} \mathbf{p}_j \mathbf{j}$ by the phase $A_{n,N} e^{2i \left(p_j + \frac{n}{2N} \right)}$, with the function $A_{n,N}$ on T defined as:

$$A_{n,N} (e^{2i p}) \stackrel{\text{def}}{=} e^{2i s n p} e^{2i N [F(p + \frac{n}{2N}) - F(p - \frac{n}{2N})]} = \sum_{m \in \mathbb{Z}} \tilde{A}_{n,N}(m) e^{2i m p} :$$

$A_{n,N}$ uniformly converges to the function a_n of Eq. (26) in the limit $N \rightarrow \infty$. For our example $F(p) = \frac{1}{2} \cos(2p)$, it takes the concise form $A_{n,N} (e^{2i p}) = e^{2i n (s p - \frac{n}{2N} \sin(2p))}$ with $\frac{n}{2N} \sin(2p) = \frac{1}{N} \sin(2p) = (1 + O((n/N)^2))$.

From there, we can express the action of \hat{P} on the quantum translations:

$$\hat{P} \hat{T}_{\frac{(m;n)}{N}} = \sum_{l \in \mathbb{Z}} \hat{T}_{\frac{(m-l;n)}{N}} \tilde{A}_{n,N}(l) = \sum_{l \in \mathbb{Z}_N} \hat{T}_{\frac{(l;n)}{N}} \tilde{A}_{n,N}^0(m-l);$$

where $\tilde{A}_{n,N}^0(m) = \sum_{l \in \mathbb{Z}} (1)^l \tilde{A}_{n,N}(m+l)$.

Therefore, \hat{P} acts on $V_{n,N}$ through the $N \times N$ Toeplitz matrix with coefficients $\tilde{A}_{n,N}^0(m)$. If we truncate this matrix to the size $\{ \mathbf{j}; \mathbf{j} \in \mathbb{Z}_N^0 \}$ with $N^0 \ll N$, we only take into account the coefficients with $\mathbf{j} \in \mathbb{Z}_N^0$. Since $A_{n,N}$ is a smooth function, each of these coefficients is the sum of a ‘‘dominant’’ term $\tilde{A}_{n,N}(m)$ and a ‘‘remainder’’. For our example, the coefficients are given by Bessel functions: $\tilde{A}_n(m) = J_{m+sn}(2n)$, and the same for $\tilde{A}_{n,N}(m)$, replacing n by $\frac{n}{N}$. These coefficients therefore satisfy $\tilde{A}_{n,N}(m) \sim C \frac{(n)^{m+nsj}}{j^{n+nsj}}$, so that the remainder is uniformly bounded above by $\frac{C^0}{N} N^{-2}$ for large N . If we call $\hat{P}_{\mathcal{J}_n,N}^1$ the truncated Toeplitz matrix with coefficients $\tilde{A}_{n,N}(m)$, we get the estimate:

$$\| \hat{P}_{\mathcal{J}_n,N} - \hat{P}_{\mathcal{J}_n,N}^1 \| \leq (2^{-1} + 1) \frac{C^0}{N} N^{-2} :$$

This estimate implies that the spectra of both matrices cannot be at a distance greater than $O((N)^{-N=4})$. The matrix $\hat{P}_{\mathcal{J}_n,N}^1$ may be analyzed on the same lines as $\hat{P}_{\mathcal{J}_n}$ in the first appendix. Its spectrum is contained for any $\epsilon > 0$ in the set $\{ \lambda > 0 \mid \text{conv} A_{n,N}(\epsilon T) \}$, which converges to set associated with a_n as $N \rightarrow \infty$.

References

- [1] O. Agam and G. Blum, *The leading Ruelle resonances of chaotic maps*, Phys. Rev. **E 62** (2000) 1977–1982
- [2] A.V. Andreev, O. Agam, B.L. Altshuler and B.D. Simons, *Semiclassical Field Theory Approach to Quantum Chaos*, Nucl. Phys. **B 482** (1996) 536–566
- [3] V.I. Arnold and A. Avez, *Ergodic Problems of Classical Mechanics*, Benjamin, 1968
- [4] V. Baladi, *Spectrum and Statisticaroperties of Chaotic Dynamics*, Progress in Math. **201** (2001) 203–223
- [5] V. Baladi and L.-S. Young, *On the spectra of randomly perturbed expanding maps*, Commun. Math. Phys. **156** (1993) 355–385; Erratum, Commun. Math. Phys. **166** (1994) 219–220
- [6] P. Bianucci, J.P. Paz and M. Saraceno, *Decoherence for classically chaotic quantum maps*, preprint quant-ph/0110033
- [7] M. Blank, G. Keller and C. Liverani, *Ruelle-Perron-Frobenius spectrum for Anosov maps*, Nonlinearity **15** (2002) 1905–1973
- [8] E.B. Bogomolny, *Semiclassical quantization of multidimensional systems*, Nonlinearity **5** (1992) 805–866
- [9] A. Böttcher and B. Silbermann, *Introduction to large truncated Toeplitz matrices*, Springer, Berlin (1999)
- [10] A. Bouzouina and S. De Bièvre, *Equipartition of the eigenfunctions of quantized ergodic maps on the torus*, Commun. Math. Phys. **178** (1996) 83–105
- [11] A.O. Caldeira and A.J. Leggett, *Influence of damping on quantum interference: An exactly soluble model*, Phys. Rev. **A 31**, 1059–1066 (1985)
- [12] C. Conley and E. Zehnder, *The Birkhoff-Lewis fixed point theorem and a conjecture of V.I. Arnold*, Invent. Math. **73**, 33–49 (1983)
- [13] I.L. Chuang and M.A. Nielsen, *Quantum Computation and Quantum Information*, Cambridge University Press (2000)
- [14] I.P. Cornfeld, S.V. Fomin and Ya.G. Sinai, *Ergodic theory*, Springer, Berlin (1982)
- [15] M. Degli Esposti, S. Graffi and S. Isola, *Classical limit of the quantized hyperbolic toral automorphisms*, Commun. Math. Phys. **167** (1995) 471–507
- [16] I. Garcia Mata and M. Saraceno, in preparation (Nov. 2002)

- [17] S. Habib, K. Shizume and W.H. Zurek, *Decoherence, Chaos and the Correspondence Principle*, Phys. Rev. Lett. **80** (1998) 4361
- [18] J.H. Hannay and M.V. Berry, *Quantization of linear maps on a torus—Fresnel diffraction by a periodic grating*, Physica **1D** (1980) 267–290; M. Degli Esposti, *Quantization of the orientation preserving automorphisms of the torus*, Ann. Inst. Henri Poincaré **58** (1993) 323–341
- [19] A. Katok and B. Hasselblatt, *Introduction to the Modern Theory of Dynamical Systems*, Cambridge University Press, 1995
- [20] J. Keating, F. Mezzadri and J. Robbins, *Quantum boundary conditions for torus maps*, Nonlinearity **12** (1999) 579–591
- [21] Yu. Kifer, *Random perturbations of dynamical systems*, Birkhäuser, Basel (1988)
- [22] M. Khodas, S. Fishman and O. Agam, *Relaxation to the Invariant Density for Kicked Rotor*, preprint nlin.CD/9910040
- [23] P. Kurlberg and Z. Rudnick, *On quantum ergodicity for linear maps of the torus*, Commun. Math. Phys. **222** (2001) 201–227
- [24] P. Kurlberg, *On the order of unimodular matrices modulo integers*, preprint math.NT/0202053
- [25] G. Lindblad, *On the generators of quantum dynamical semigroups*, Commun. Math. Phys. **48** (1976) 119–130
- [26] C. Manderfeld, J. Weber and F. Haake, *Classical versus Quantum Time Evolution of Densities at Limited Phase-Space Resolution*, preprint nlin.CD/0107020; J. Weber, F. Haake, P.A. Braun, C. Manderfeld and P. Šeba, nlin.CD/0105047
- [27] J. Marklof and Z. Rudnick, *Quantum unique ergodicity for parabolic maps*, Geometric and Functional Analysis **10** (2000) 1554–1578
- [28] S. Nonnenmacher and M.R. Zirnbauer, *Det-det Correlations for Quantum Maps: Dual Pair and Saddle-Point Analyses*, J. Math. Phys. **43**, 2214–2240 (2002)
- [29] A.M. Childs, I.L. Chuang and D.W. Leung, *Realization of quantum process tomography in NMR*, Phys. Rev. **A 64**, 012314 (2001); L.M.K. Vandersypen *et al.*, *Experimental realization of Shor’s quantum factoring algorithm using nuclear magnetic resonance*, Nature **414**, 883–887 (2001)
- [30] W. Parry and M. Pollicott, *Zeta functions and the periodic orbit structure of hyperbolic dynamics*, Astérisque, vol. 187–188, Société mathématique de France, Paris, 1990
- [31] I. Percival and F. Vivaldi, *Arithmetical properties of strongly chaotic motions*, Physica **25D** (1987) 105–130

- [32] T. Prosen, *Chaotic resonances in quantum many-body dynamics*, preprint (2002)
- [33] M. Reed and B. Simon, *Methods of modern mathematical physics, I: Functional Analysis*, Academic Press, 1972
- [34] D. Ruelle, *Locating Resonances for Axiom A Dynamical Systems*, J. Stat. Phys. **44**, 281–292 (1986); *One-dimensional Gibbs states and Axiom-A diffeomorphisms*, J. Diff. Geom. **25**, 117–137 (1987)
- [35] H.H. Rugh, *The correlation spectrum for hyperbolic analytic maps*, Nonlinearity **5**, 1237–1263 (1992); *ibid*, *Generalized Fredholm determinants and Selberg zeta functions for Axiom A dynamical systems*, Ergod. Theory Dynam. Syst. **16**, 805–819 (1996)
- [36] M. Tabor, *A semiclassical quantization of area-preserving maps*, Physica **6D** (1983) 195–210
- [37] K. Takahashi, *Distribution in Classical and Quantum Mechanics*, Prog. Theor. Phys. Suppl. **98** (1989) 109–156
- [38] S. Zelditch, *Index and dynamics of quantized contact transformations*, Ann. Inst. Fourier, **47** (1997) 305–365